SEDIMENTOLOGY the journal of the International Association of Sedimentologists

Sedimentology (2010) **57,** 642–669 doi: 10.1111/j.1365-3091.2009.01111.x

The incised valley of Baffin Bay, Texas: a tale of two climates

ALEXANDER R. SIMMS*, NIRANJAN ARYAL*[1], LAUREN MILLER* and YUSUKE YOKOYAMA†‡

**Boone Pickens School of Geology, Oklahoma State University, 105 NRC, Stillwater, OK 74078, USA (E-mail: alex.simms@okstate.edu)*

†Ocean Research Institute and Department of Earth and Planetary Sciences, University of Tokyo, 1-15-1 Minamidai, Nakano-ku, Tokyo 164-8639, Japan

‡Institute of Biogeosciences, Earth and Life History Research, Japan Agency for Marine-Earth Science and Technology, Japan

Associate Editor – Dave Mallinson

ABSTRACT

Baffin Bay, Texas is the flooded Last Glacial Maximum incised valley of the Los Olmos, San Fernando and Petronila Creeks along the north-western Gulf of Mexico. Cores up to 17 m in length and high-resolution seismic profiles were used to study the history of Baffin Bay over the last 10 kyr and to document the unusual depositional environments within the valley fill. The deposits of the Baffin Bay incised valley record two major and two minor events. Around 8·0 ka, the estuarine environments backstepped more than 15 km in response to an increase in the rate of sea-level rise. Around 5·5 ka, these estuarine environments changed from environments similar to other estuaries of the northern Gulf of Mexico to the unusual suite of environments found today. Another minor flooding event occurred around 4·8 ka in which several internal spits were flooded. Some time after 4·0 ka, the upper-bay mud-flats experienced a progradational event. Because of its semi-arid climate and isolation from the Gulf of Mexico, five depositional environments not found in the other incised-valley fills of the northern Gulf of Mexico are found today within Baffin Bay. These deposits include well-laminated carbonate and siliciclastic open-bay muds, ooid beaches, shelly internal spits and barrier islands, serpulid worm-tube reefs and prograding upper-bay mud-flats. Based on these unusual deposits, and other characteristics of Baffin Bay, five criteria are suggested to help identify incised valleys that filled in arid and semi-arid climates. These criteria include the presence of: (i) hypersaline-tolerant fauna; (ii) aeolian deposits; and (iii) carbonate and/or evaporite deposits; and the absence of: (iv) peat or other organic-rich deposits in the upper bay and bay-margin areas; and (v) well-developed fluvially dominated bayhead deltas.

Keywords Climate change, estuary, Gulf of Mexico, Holocene, incised valley, sequence stratigraphy, transgression.

INTRODUCTION

Incised valleys are an important element within conventional hydrocarbon systems and are capable of documenting environmental changes. As a result, a number of studies have been designed to model their fill and stratigraphic architecture (Zaitlin *et al.*, 1994; Dabrio *et al.*, 2000; Anthony *et al.*, 2002; Mallinson *et al.*, 2005; Boyd *et al.*, 2006; Simms *et al.*, 2006). Studies on incised-valley fill range from Late Quaternary and modern systems, which flooded to form estuaries (Nichols

[1]Present address: Schlumberger, 1325 S. Dairy Ashford, Houston, TX 77077, USA.

et al., 1991; Allen & Posamentier, 1993; Ashley & Sheridan, 1994; Thomas & Anderson, 1994; Nordfjord *et al.*, 2006; Rodriguez *et al.*, 2008), to those preserved in the fossil record and studied in outcrop and sub-surface (Martinsen, 1994; Feldman *et al.*, 1995; Ye & Kerr, 2000; Ardies *et al.*, 2002; Bowen & Weimer, 2003; Rossetti & Junior, 2004). Models of incised-valley fill typically consist of a landward segment filled mostly with fluvial deposits, a middle segment of fluvial deposits overlain by central-basin deposits and a seaward segment of fluvial deposits at the base overlain by central-basin deposits and capped by marine deposits (Zaitlin *et al.*, 1994).

Recent studies have expanded upon the Zaitlin *et al.* (1994) model of incised-valley fill. These expansive models highlight the importance of fluvial processes and produce fill-models almost completely composed of fluvial deposits (Harris, 1994; Garrison & Van den Bergh, 2006; Li *et al.*, 2006). Other studies have shown that some incised valleys are not filled completely by sediments before the transgressive shoreline passes through or are excavated again during the transgression leaving accommodation on the shelf that is later filled with open-marine deposits such as shelf dunes (Payenberg *et al.*, 2006) or sediment gravity flows (Thieler *et al.*, 2007). However, most available case-studies of Late Quaternary and modern incised-valley systems are biased towards wetter climates and few studies provide examples of the impact of climate variability on the type of fill that can form within incised valleys. As a result, little is known about the stratigraphic architecture of incised valleys that formed within arid and semi-arid climates. The purpose of this study was to: (i) summarise previous work conducted on the sediments of Baffin Bay, Texas, USA; (ii) present new data documenting the history of the system; and (iii) provide a depositional model for the incised valley as a whole. This study provides one of the few Quaternary examples of an incised valley filled within a semi-arid or arid climate and provides criteria for recognising incised valleys filled within arid and semi-arid climates.

STUDY AREA

Geomorphic setting

Baffin Bay is located in the north-western corner of the passive margin of the Gulf of Mexico (Fig. 1). The coastal plain has a low gradient, averaging less than 0·8 m/km over the final 80 km. The shoreline of the lower portion of the bay is rimmed by shallow tidal flats and low beach ridges, which give way to low bluffs 2 to 4 m high in the upper reaches of the bay. Unlike most estuaries of the Gulf of Mexico, Baffin Bay is not connected to the open Gulf of Mexico via a tidal inlet, but is completely isolated from the open Gulf by the 180 km long Padre Island, the longest barrier island in the world (Fig. 1). Baffin Bay proper is further isolated from the adjacent Laguna Madre (Fig. 1) by a series of shallow reefs at the mouth of the bay (Fig. 2). Fisk (1959) studied Padre Island and Laguna Madre and placed their formation at around 5·0 ka. Prior to 5 ka, Baffin Bay probably maintained a better connection with the Gulf of Mexico.

Sea-level controls

The incised valleys of the Gulf of Mexico formed in response to a drop in sea-level from Marine Isotope Stage (MIS) 5e, at 120 ka, to MIS2, at 20 ka (Simms *et al.*, 2006, 2007a). Prior to this drop in sea-level, the Ingleside barrier ridge formed in response to the MIS5e highstand. The Ingleside barrier ridge is a topographically high sandy ridge that runs parallel to the modern coastline with a maximum elevation of approximately 5 to 9 m above sea-level (Price, 1933a; Paine, 1993; Otvos & Howat, 1996; Otvos, 2005). The Ingleside barrier ridge terminates immediately to the north of the study area; aeolian processes have probably removed this feature around Baffin Bay (Price, 1933a). The rivers of the north-western Gulf of Mexico responded to the episodic fall in sea-level between 120 and 20 ka by forming several terraces (Price, 1933a), termed 'Deweyville terraces', along the margins of their valleys (Bernard, 1950; Blum *et al.*, 1995; Durbin *et al.*, 1997). However, because their ages do not necessarily correspond from valley to valley, Otvos (2005) suggested that other factors, including differences in climate, may have contributed to the formation of the 'Deweyville' terraces. The total sea-level fall during the Last Glacial Maximum, which occurred at 20 ka, is thought to have been between 90 and 120 m (Curray, 1960; McFarlan, 1961; Scott *et al.*, 1998; Roberts *et al.*, 2004; Simms *et al.*, 2007b). The San Fernando, Petronila and Los Olmos Creeks (Fig. 1) responded to this sea-level fall by excavating the valley that has now flooded to form Baffin Bay and its three tributary bays (Fisk, 1959; Behrens, 1963). Behrens (1963) interpreted a series of small steps in seismic profiles as buried

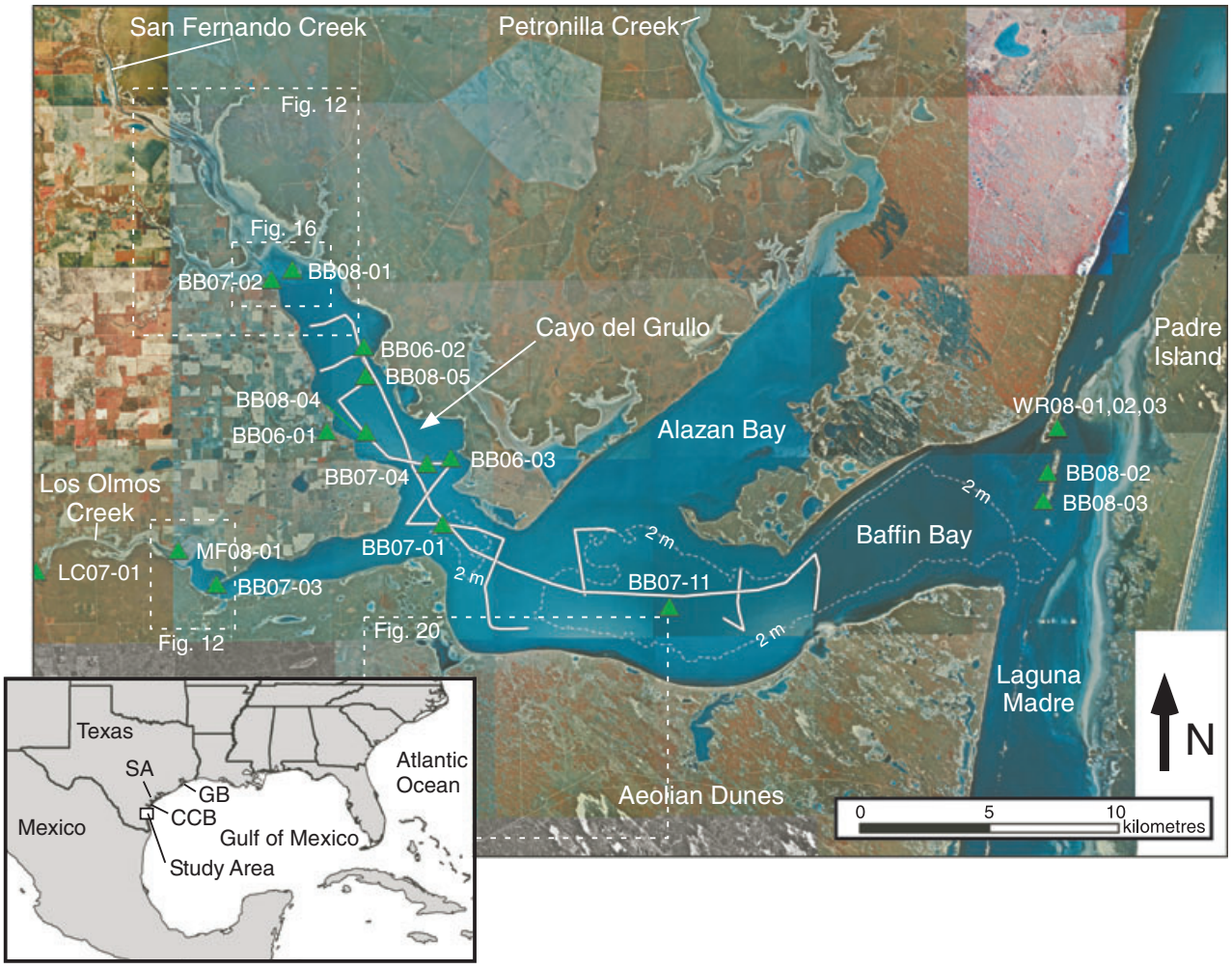

Fig. 1. Location of the study area within the Gulf of Mexico as well as data collected as part of this study. For inset map, GB is Galveston Bay, SA is San Antonio Bay, CCB is Corpus Christi Bay. Aerial photographs courtesy of the Texas Natural Resources Information System (http://www.tnris.state.tx.us).

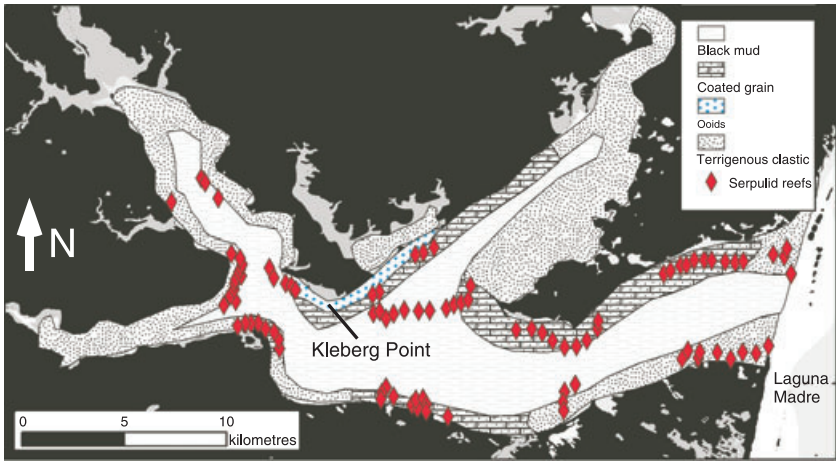

Fig. 2. Distribution of modern sediments of Baffin Bay as mapped by Dalrymple (1964) and Andrews (1964).

fluvial terraces beneath Baffin Bay but no cores have confirmed a fluvial origin for the small steps.

The Holocene transgression over the last 10 kyr is thought to have been slow and continuous within the north-western Gulf of Mexico (Shepard, 1960; Tornqvist *et al.*, 2004a) with the exception of possible abrupt increases in the rate of sea-level rise between 8 and 10 ka (Tornqvist

et al., 2004b; Milliken *et al.*, 2008a). The presence of high-order fluctuations and possible mid-Holocene highstands within the north-western Gulf of Mexico is arguable (Morton *et al.*, 2000; Otvos, 2001), with supporting evidence both for (Tanner *et al.*, 1989; Blum *et al.*, 2001; McBride *et al.*, 2007) and against this hypothesis (Otvos, 2004; Wright *et al.*, 2005; Rodriguez & Meyer, 2006). Although hydro-isostatic tilting can cause mid-Holocene highstands (Yokoyama *et al.*, 1996), most current models of hydro-isostacy do not predict a mid-Holocene highstand for the Gulf of Mexico (Simms *et al.*, 2007b). Simms *et al.* (in press) examine the evolution of seven shallow ponds at elevations between −0·8 and +0·8 m above sea-level on the southern margins of Baffin Bay and find no evidence for sea-levels above +0·4 m over the last 5·6 kyr.

Hydrology and climate

Baffin Bay receives, on average, between 60 and 80 cm $year^{-1}$ of precipitation (Behrens, 1966). Evaporation exceeds precipitation by about 60 cm $year^{-1}$ (Behrens, 1966) and, as a result of its semi-arid setting and isolation, the bay is hypersaline with average salinities of 40 to 50. However, salinities have reached as high as 85 during drought years (Behrens, 1966) and as low as 2 after cloudbursts (Gunter, 1945). The three creeks that flow into Baffin Bay-Los Olmos Creek, San Fernando Creek and Petronila Creek-drain a total of 11 200 km^2. The creeks deliver variable amounts of water and sediment to the bay. The average annual discharge for Los Olmos Creek from 1969 to 2008, based on a USGS stream gauge approximately 40 km inland from Baffin Bay, was 0·12 $m^3 s^{-1}$ (United States Geological Survey, 2009). The highest average annual stream flow reported during that time period was 0·95 $m^3 s^{-1}$ while the lowest was 0·0 $m^3 s^{-1}$ (United States Geological Survey, 2009). A stream gauge approximately 60 km inland from Baffin Bay on San Fernando Creek reported an average annual stream flow of 0·64 $m^3 s^{-1}$ between 1966 and 2008 with a high of 3·53 $m^3 s^{-1}$ and a low of 0·03 $m^3 s^{-1}$ (United States Geological Survey, 2009). No data are available for Petronila Creek. Modern drainage of these creeks, particularly to the south of Baffin Bay, is disrupted by aeolian dunes. Thus, the delivery of sediment to Baffin Bay from these creeks today is sporadic and limited to intense rain events.

Within the adjacent Laguna Madre, the high salinities have resulted in the precipitation of gypsum and other salts in shallow tidal flats and playas, although the salts are usually removed during rainstorms (Rusnak, 1960). As a consequence of the dry climate, the soils within the area contain higher amounts of $CaCO_3$ than areas to the north and east (Driese *et al.*, 2005) and thick caliche deposits have formed around Baffin Bay (Price, 1933b). The caliche acts as a shoreline stabiliser when compared with other Gulf of Mexico bay margins. As a result, Baffin Bay has retained its dendritic character (Behrens, 1963; Fig. 1).

Continuous strong winds blow from the south-east at an average of 15 to 24 km h^{-1} for seven months of the year, from spring through to autumn (Rusnak, 1960). When winter fronts pass through, the wind shifts to the north-west (Lohse, 1956). As a result of the strong winds and low astronomical tidal range (<0·1 m), meteorological conditions including precipitation events are more important than astronomical tides in controlling water-level oscillations (Breuer, 1957; Militello, 1998). Hurricanes strike the central Texas coast about four times every 30 years (Elsner & Kara, 1999).

Previous work

Dalrymple (1964) conducted the most exhaustive study of the modern environments of Baffin Bay, but did not sample the upper reaches of the three tributary bays. Dalrymple (1964) found four major categories of sediments along the bay floor; black-mud, ooids, quartz-mollusc sands and coated-grains (Fig. 2). Alaniz & Goodwin (1974) conducted a sediment survey of Cayo de Grullo and confirmed most of the observations by Dalrymple (1964). Freeman (1962), Dalrymple (1964) and Land *et al.* (1979) studied the formation of modern ooids in Baffin Bay and nearby Laguna Madre. These authors found that the ooids in Baffin Bay have three types of coatings reflecting the energy conditions of their formation, chemistry and crystallography. Behrens (1963) conducted one of the first seismic surveys of Baffin Bay and provided a rough map of the axis of the incised valley. Behrens (1974) summarised the work conducted on the bay up to that time focusing on four environments characteristic of the bay: (i) algal mat laminar muds; (ii) oolitic beach sands; (iii) serpulid reefs; and (iv) carbonate muds. Behrens (1974) also provided a short summary of the evolution of the bay noting that the formation of Padre Island around 5 ka had a significant impact on the history of the bay.

METHODS

A total of 18 cores with lengths up to 17 m were collected within Baffin Bay. In addition, 65 km of high-resolution seismic data, mostly from upper Baffin Bay, was collected. The locations of the cores and seismic profiles are shown in Fig. 1. In addition, several of the modern environments were visited and photographed in the field. All seismic profiles, cores and other observations were correlated and maps constructed using ArcMap 9.2 software.

Cores

Two different diameter cores were collected in Baffin Bay. Thirteen, 7.6 cm diameter cores up to 4·2 m in length were collected using a portable vibracore rig and a tripod or davit aboard the *R/V Trinity*. Five longer 5·1 cm diameter cores were collected using a combination push-rotary rig aboard the *R/V Trinity*. These cores were taken in 1·5 m sections to a depth of 17·7 m. Cores were refrigerated and sectioned at the Oklahoma State University laboratory. One-half of the core was set aside for archival purposes and the other half was sampled. The cores were described according to grain size, sorting, sedimentary structures and macrofauna. Grain-size analysis was conducted on most cores at 15 to 20 cm intervals using a CILAS1180L laser diffraction particle-size analyser (CILAS Particle Size, Madison, WI, USA). Approximately 4 cm^3 of material was soaked overnight using a mild detergent to disaggregate the clays. One hundred and ninety-eight samples were run using a 60 sec ultrasonic stimulation following the methods of Sperraza *et al.* (2004). In addition, to determine the mineralogy of white laminations within the cores, nine samples were taken for powder X-ray diffraction using a Phillips Electronics PW3710 (PANalytical BV, Almelo, the Netherlands) at Oklahoma State University. X-ray peaks of the dried and crushed sediment samples were compared with peaks of known minerals for identification.

Seismic

Approximately 65 km of high-resolution seismic profiles were collected from the bay. An Octopus 360+ Sub-bottom Acquisition System (CodaOctopus Products Limited, Edinburgh, UK) was used during data collection. An Applied Acoustic Engineering AA200 boomer plate (Applied Acoustic Engineering Limited, Great Yarmouth, UK) with a power setting of 200 joules was used as a source. An Applied Acoustic Engineering AH360/8 towed hydrophone array with a hydrophone spacing of 0·365 m was used as the receiver. A 10-millisecond (ms) linear sweep from 1·5 to 7 kHz was used to provide a vertical resolution of a few decimetres. As the seismic survey was single channel, the only processing necessary was the application of simple band-pass filters (100 and 400 Hz) and automatic gain control. Location of track lines was provided using a GPS system.

RESULTS

Seismic

The seismic data from Baffin Bay were used to construct a map of the interpreted Last Glacial Maximum unconformity (Fig. 3). This surface

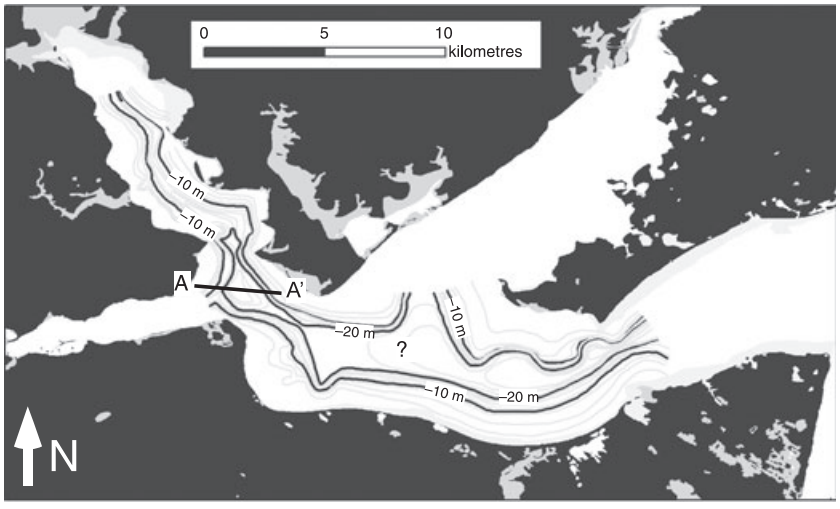

Fig. 3. Map of the Last Glacial Maximum unconformity beneath Baffin Bay as determined in seismic profiles.

was picked as a truncation of lower reflections that were onlapped by overlying reflections (Fig. 4). A two-way travel time (TWTT) seismic velocity of 1500 m s^{-1} was assumed based on previous studies (Shideler, 1986; Sydow & Roberts, 1994; Anderson *et al.*, 2004; Milliken *et al.*, 2008b). Good correlation of sedimentary contacts with seismic contacts was found using this velocity. The Last Glacial Maximum unconformity probably correlates with the sequence boundary mapped offshore by several authors summarised by Simms *et al.* (2007a). Eckles *et al.* (2004) and Simms *et al.* (2007a) mapped a lowstand valley on the shelf that appears to be the seaward extension of the Baffin Bay incised valley. The quality of the seismic profiles from the lower portions of the bay was not as good as that from the upper reaches of the bay because of the higher wave energies associated with a longer fetch. Thus, the interpretations of the Last Glacial Maximum unconformity are not as robust in the lower reaches of the bay.

Above the interpreted Last Glacial Maximum unconformity, six seismic facies were identified (Fig. 5). Sedimentary facies were used to ground truth the interpretation of the seismic facies. These seismic facies and their distribution were used as a basis for the construction of the stratigraphic architecture of the incised-valley fill (Fig. 6). A summary of these seismic facies with their corresponding sedimentary facies and interpreted depositional environment is given in Table 1.

Seismic facies A

Seismic facies A consists of high-amplitude horizontal parallel, closely spaced reflections (Fig. 5). It is found mostly in the top portions of the seismic profiles. Cores sampling this facies contained sedimentary facies 4, 5 and 6. Based on its geographic location near the surface of the middle portions of the bay and the sedimentary facies it sampled, seismic facies A is interpreted as representing an open-bay environment.

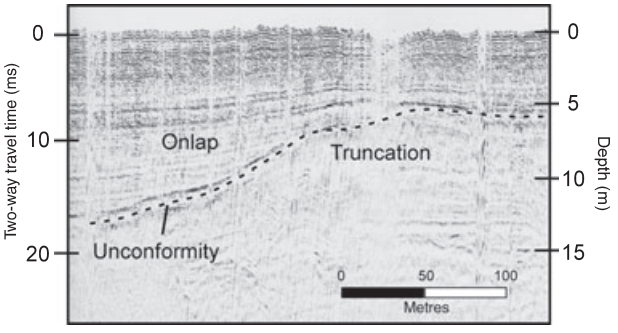

Fig. 4. Illustration of the relationship of reflections to the surface picked as the Last Glacial Maximum unconformity.

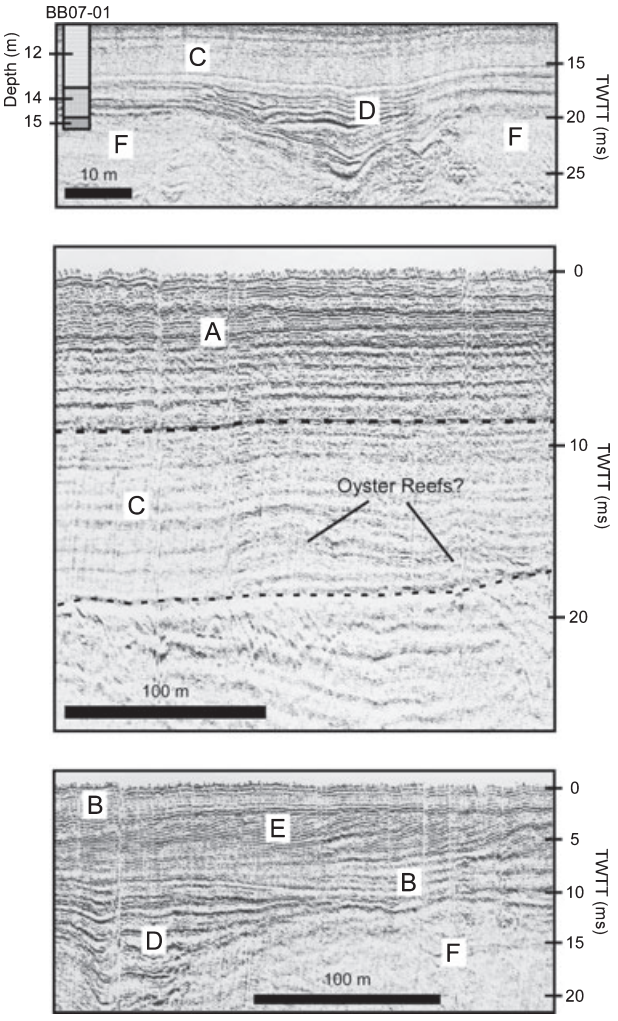

Fig. 5. Examples of seismic facies identified within this study. See Table 1 for interpretations of seismic facies 'A' to 'F'. TWTT, two-way travel time.

Seismic facies B

Seismic facies B consists of continuous, low to medium amplitude parallel reflections (Fig. 5). The reflections in seismic facies B are not as smooth and horizontal as those of seismic facies A. Cores that sample this seismic facies contain sedimentary facies 3, 4 and 5. It dominates the shallow portions of seismic profiles from the upper reaches of the bay. Based on its geographic position and the sedimentary facies associated with seismic facies B, it is interpreted as representing an upper-bay environment.

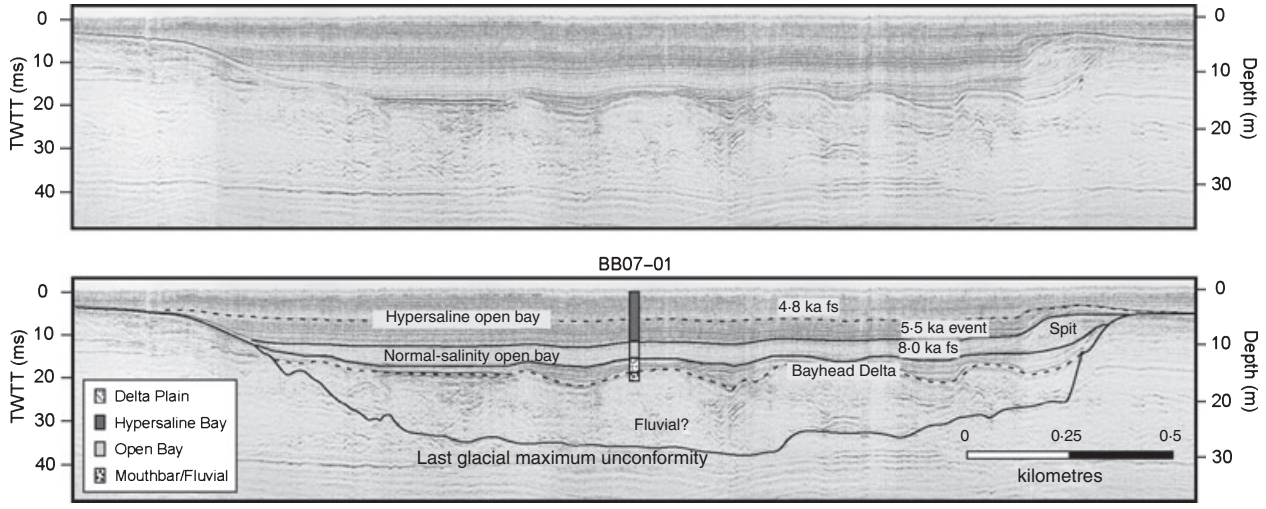

Fig. 6. Uninterpreted and interpreted seismic profile through the incised valley of Baffin Bay. See Fig. 3 for seismic profile location. fs, flooding surface; TWTT, two-way travel time.

Table 1. Seismic facies and equivalent sedimentary facies with their interpretation. See Table 2 for a description of the sedimentary facies.

Seismic facies	Characteristics	Sedimentary facies equivalent	Interpreted environment
A	Horizontal, parallel, closely spaced medium-high amplitude continuous reflections	4, 5, 6	Open bay
B	Continuous, low–medium amplitude parallel reflections	3, 4, 5	Upper-bay
C	Very low amplitude continuous, parallel to subparallel reflections	12	Open-bay (wetter)
D	High-amplitude, continuous wavy reflections with isolated v-shaped reflection packages (small channels)	13, 14	Bayhead delta plain
E	Sigmoid-oblique reflections	7	Fetch-limited spits
F	Choatic, low-amplitude reflections	15	Bayhead delta/river

Seismic facies C

Seismic facies C is only found in the deeper portions of the seismic profiles. It consists of very low amplitude to transparent continuous parallel to sub-parallel reflections (Fig. 5). Seismic facies C also contains mounds of higher amplitude parallel reflections (Fig. 5) similar to those found in Corpus Christi Bay about 50 km north of Baffin Bay (Morton & Kindinger, 1998; Simms *et al.*, 2008). Simms *et al.* (2008) sampled the flanks of one of these mounds in Corpus Christi Bay and found several *Crassostrea virginica* shells (oysters). These mounds were interpreted by Simms *et al.* (2008) and Morton & Kindinger (1998) to represent oyster reefs. Cores from Baffin Bay that sample seismic facies C contain sedimentary facies 12. Based on the presence of oyster reefs and the characteristics of the sedimentary facies associated with it, seismic facies C is interpreted as representing open-bay deposits similar to those found in Corpus Christi Bay (Morton & Kindinger, 1998; Simms *et al.*, 2008).

Seismic facies D

Seismic facies D consists of high-amplitude, continuous wavy reflections with isolated v-shaped reflection packages (Fig. 5). Cores that sample seismic facies D contain sedimentary facies 13 and 14. The isolated v-shaped reflection packages within seismic facies D appear to truncate seismic facies F. Based on its position within the fill and the characteristics of the associated sedimentary facies 13 and 14, seismic facies D is

interpreted as representing a bayhead delta-plain environment. The v-shaped reflection packages are interpreted as representing distributary channels within the delta plain.

Seismic facies E

Seismic facies E consists of sub-parallel oblique to sigmoid oblique reflections (Fig. 5). The packages have the appearance of clinoform packages suggesting progradation (Figs 5 and 7). Two possible environments could produce prograding clinoform packages within an estuary: lobes of a bayhead delta or spits. Several attempts were made to sample the deeper, clearer seismic examples of the prograding packages. However, the only material recovered during the attempts was a few sand grains and shell fragments, not enough for an unambiguous interpretation. One ill-defined prograding package was sampled using a shallow vibracore (Fig. 7). It contains a shelly sand similar in character to the facies recovered in the cores from modern spits (facies 7, Table 1; Fig. 7); this, coupled with their attachment to the incised-valley walls (Fig. 6), favours a buried spit interpretation over a bayhead delta interpretation. A map of the distribution of these spit deposits in the sub-surface of upper Baffin Bay is shown in Fig. 8.

Seismic facies F

Seismic facies F consists of chaotic, low-amplitude reflections (Fig. 5). This seismic facies is only found in the deeper portions of the seismic profiles (Figs 5 and 6). In many locations it is truncated and overlain by seismic facies D. Core BB07-01 sampled the sedimentary deposits associated with seismic facies D and F. The core contains sedimentary facies 15 within seismic facies F. It is interpreted as representing either the mouth bar of a bayhead delta or other fluvial deposits.

Cores

A total of 15 facies were identified within the cores from Baffin Bay. A summary of these facies and their interpreted depositional environment is shown in Table 2. Select facies from cores are illustrated in Figs 9 and 10. These 15 facies can be grouped into two facies assemblages.

Facies assemblage 1

Facies assemblage 1 represents the deposits of the modern environments of Baffin Bay. Nine modern environments are found within Baffin Bay and their deposits represent 11 of the 15 facies identified within the cores. These modern environments include a fluvial system, mud-flat, upper bay, open bay, 'fetch-limited' spit/barrier island, worm-tube reef, washover/lower bay, barrier island and ooid beaches. Each one of these environments is associated with at least one facies. Four of these modern environments found within the Baffin Bay system are not common to other well-studied Quaternary incised valleys (for example, Gironde Estuary, Galveston Bay, Chesapeake Bay, etc.). These four modern environments include ooid beaches, serpulid worm-tube reefs, internal or 'fetch-limited' shelly spits and barrier islands, and mud-flats.

Fluvial system. Two sedimentary facies, facies 1 and 2, are found within the modern fluvial systems of the creeks flowing into Baffin Bay.

Sedimentary facies 1: Sedimentary facies 1 represents the modern floodplain deposits of the creeks flowing into Baffin Bay. It consists of a light greenish-grey clay with few distinct sedimentary structures or fauna preserved in cores (Fig. 9). The sedimentary features found within this facies include plant material and darker-clay laminae (<1 cm). It lacks foraminifera and mollusc shells.

Sedimentary facies 2: Sedimentary facies 2 represents the modern creek-channel deposits. It consists of a brownish-grey, poorly sorted upper fine sand without any sedimentary structures or fauna preserved within the core (Fig. 9). The poorly sorted sand does contain plant fragments and gravel. The gravel component contains rounded caliche nodules.

Mud-flats. Unlike the other bays in the northwestern Gulf of Mexico (Fig. 11), no bayhead delta has prograded into Baffin Bay (Fig. 12). Instead of fluvial-dominated bayhead deltas, the upper reaches of Baffin Bay are filling with mud-flats (Fig. 12). These mud-flats are similar to the tidal-flats and mud-flats of Laguna Madre, Texas (Rusnak, 1960; Miller, 1975) and many other tide-dominated estuaries and other macrotidal coasts (Coleman & Wright, 1978; Alexander *et al.*, 1991; Dalrymple *et al.*, 1992; Yang *et al.*, 2005). However, the 'tidal creeks' that drain them are very shallow (a few centimetres) and more subdued than in other coasts. In addition, unlike the bayhead deltas of most estuaries (Fig. 11), these mud-flats have only one fluvial channel and lack the network of distributary channels common to most fluvial-

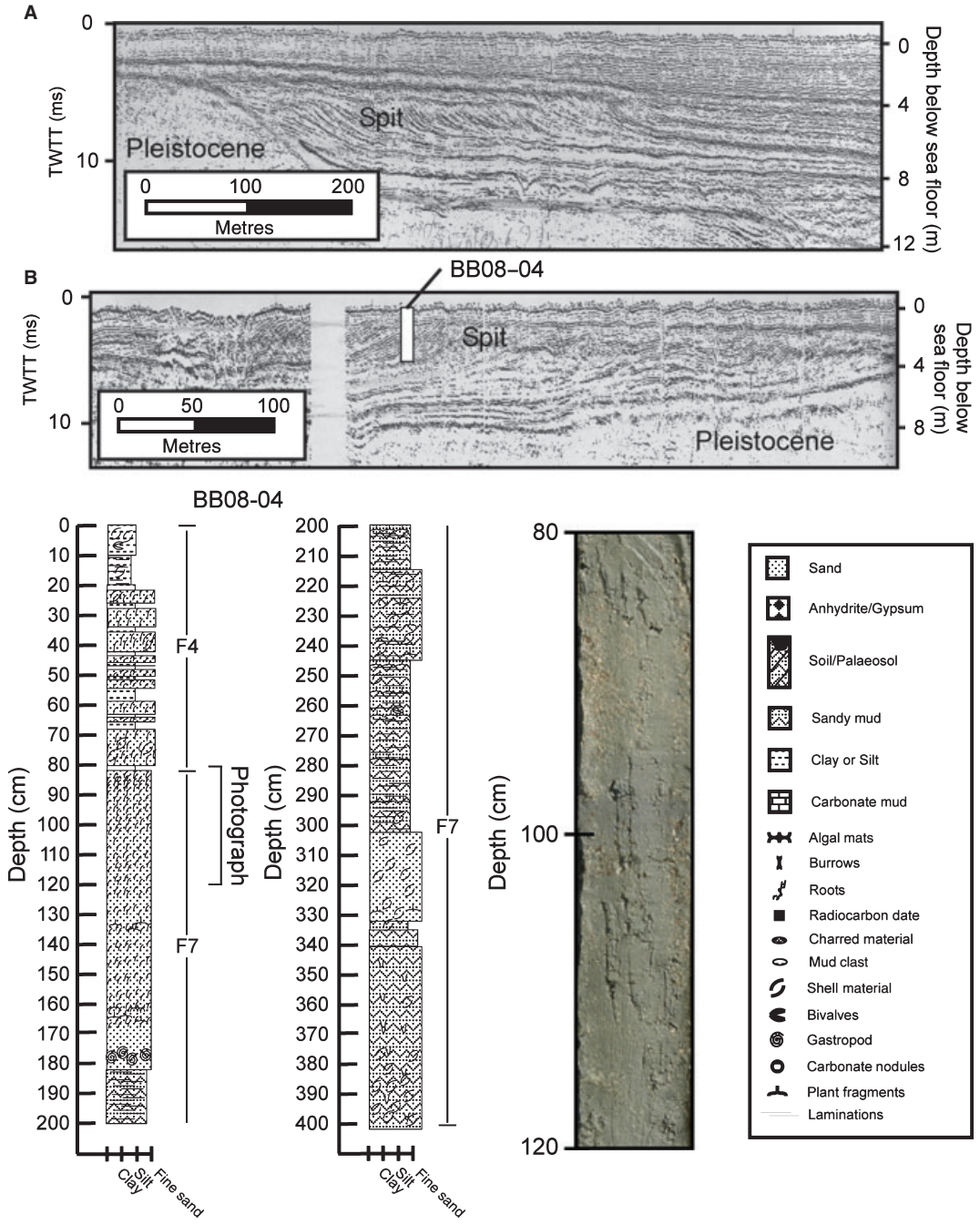

Fig. 7. Two seismic profiles (A) and (B) through the prograding clinoform packages interpreted as representing buried spit deposits. Also shown is the description and a photograph of a core taken through one of the prograding clinoform packages. See Fig. 8 for seismic line locations.

dominated bayhead deltas (Fig. 12). In addition, no sandy mouth bar deposits are found within these mud-flats.

Another distinct characteristic of these mud-flats is the prevalence of large expanses of algal mats (Fig. 13). A core through one of the mud-flats illustrates two key characteristics of the mud-flat deposits: algal mats and carbonate nodules (Fig. 12). The algal mats are composed of blue-green algae (Behrens & Frishman, 1971); they result in laminations of algal material and mineralogenic sand. The algal mats are periodically inundated when strong winds blow from the south-east, usually from the spring to early autumn. When the wind subsides, the mud-flats are exposed. This is when pedogenic processes

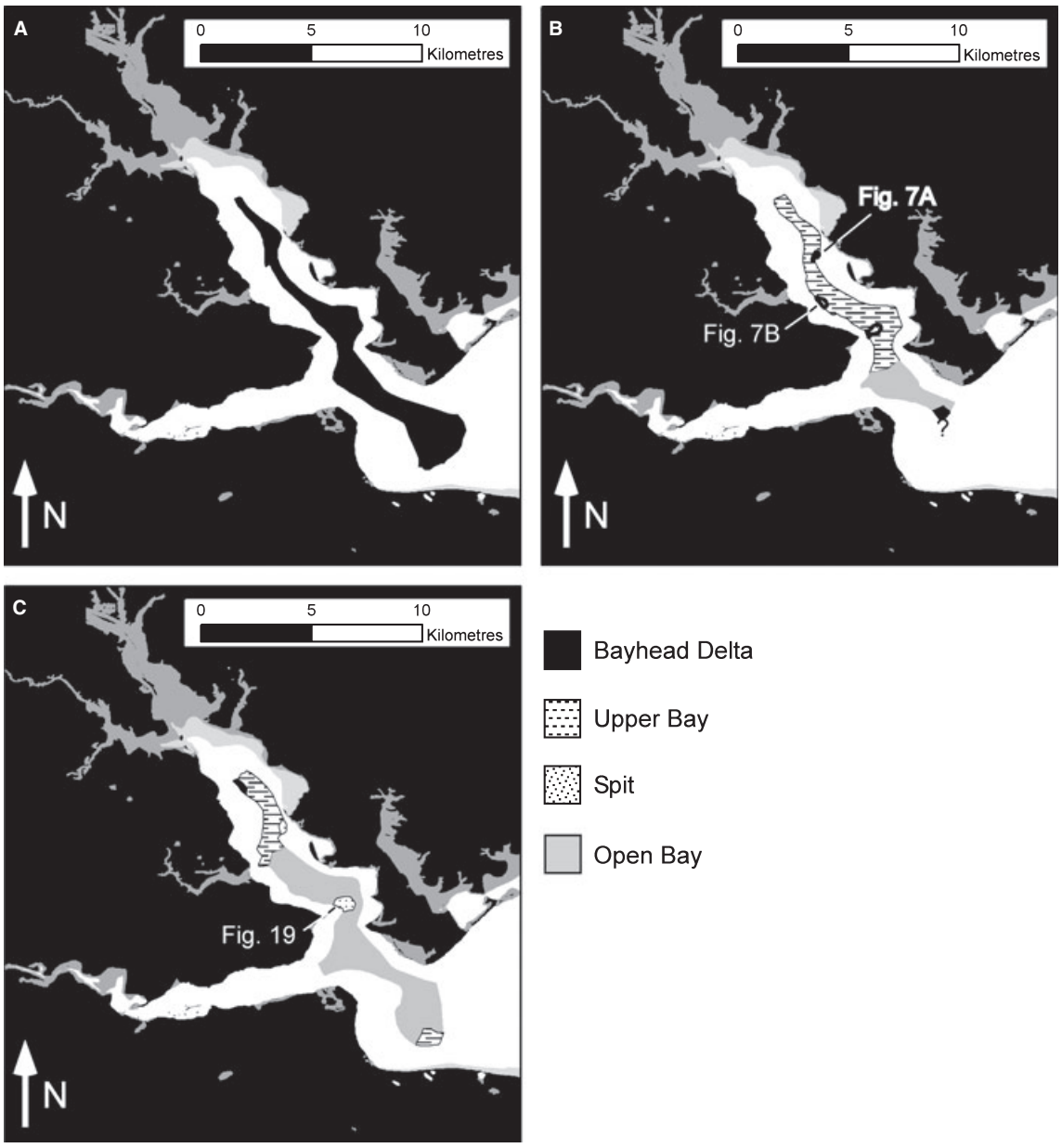

Fig. 8. Palaeogeographic maps for: (A) upper Baffin Bay before 8·0 ka; (B) upper Baffin Bay after the 8·0 flooding event; and (C) upper Baffin Bay after 5·5 ka but before 4·8 ka. Note the distribution of spits in the sub-surface of Baffin Bay.

probably operate on the mud-flats and leach and precipitate the calcium carbonate to form the carbonate nodules. A core from the modern mud-flats contains a distinctive facies: sedimentary facies 3.

Sedimentary facies 3: Sedimentary facies 3 consists of light to dark grey clayey silt/silt with some dolomite and algal laminae (Figs 9 and 12). It also contains burrows and *in situ* carbonate nodules and plant fragments. *Anomalocardia cuneimeris*, a mollusc that inhabits hypersaline lagoons (Andrews, 1971), is found occasionally within these deposits. This facies is also found in several of the longer cores taken from the centre of Baffin Bay (Fig. 9).

Upper bay. The upper bay portions of Baffin Bay are similar to other upper-bay environments of the north-western Gulf of Mexico These deposits are characterized by sedimentary facies 4.

Sedimentary facies 4: Sedimentary facies 4 consists of dark greenish-grey muddy sand with more than 50% very fine sand or silt with several sand laminae. The facies contains the molluscs

Table 2. Summary of the sedimentary facies and their interpretation.

Facies no.	Short description	Interpretation
1	Green stiff clay with few organics	Modern fluvial floodplain
2	Brown sand with plant fragments and gravel	Modern fluvial system
3	Mud with algal mats and carbonate nodules	Mud flat
4	Muddy sand with shells	Upper bay/bay margin
5	Homogenous mud	Open bay or distal upper bay
6	Well laminated mud	Dry-climate open bay
7	Sandy shell hash/shelly sand	'Fetch-limited' spit/barrier island
8	Well-sorted clean carbonate-rich sand	Barrier-island sands
9	Shelly sand with gastropods	Grass flat around serpulid reef
10	Worm-tube and shell fragments	Distal worm-tube reef facies
11	Green well-sorted sand without shells	Pleistocene barrier island
12	Shelly mud with diversity of molluscs	Wet-climate open bay
13	Stiff dark bluish-grey clay	Fluvial floodplain
14	Organic sandy mud with plant material	Delta plain
15	Fine sand with plant material and shells	Bayhead delta mouthbar/fluvial

Mulinia lateralis and *Anomalocardia cuneimeris*. It also contains foraminifera and plant fragments. Based on its presence in the core tops from the upper bay and bay margins, sedimentary facies 4 is interpreted to represent an upper-bay/bay-margin environment.

Open bay. The bulk of the sedimentary fill within the Baffin Bay incised valley is grey clayey-silt (Figs 14 and 15). However, the grey clayey-silt from the open-bay of Baffin Bay is different from other open-bay deposits found in Corpus Christi Bay (Simms *et al.*, 2008), Galveston Bay (Anderson *et al.*, 2008), Matagorda Bay (Maddox *et al.*, 2008) and elsewhere. The main difference is the presence of carbonate mud laminae (Fig. 9). The carbonate mud is composed of aragonite, magnesium calcite and dolomite and is thought to be deposited during drought periods in which the salinities exceed 60 ppt (Behrens & Land, 1972; Behrens, 1974) or in the presence of sulphate reduction (Morse *et al.*, 1992). In addition, in Corpus Christi Bay (Simms *et al.*, 2008), Galveston Bay (Anderson *et al.*, 2008) Matagorda Bay (Maddox *et al.*, 2008) and elsewhere, the open-bay deposits are devoid of sedimentary structures such as laminae or are highly bioturbated (Shepard & Moore, 1960; Gingras *et al.*, 1999). However, in Baffin Bay, the hypersaline conditions, hypoxic environment at the sediment–water interface and instability of the substrate discourage its colonisation by bottom dwellers and thus reduces bioturbation (Rusnak, 1960; Dalrymple, 1964; Behrens, 1974); this results in areas of well-laminated sediments within the open-bay environment. Similar laminations are found within shallow lagoonal deposits behind the many spits that form along the margins of Baffin Bay. The modern open bay consists of two sedimentary facies.

Sedimentary facies 5: Sedimentary facies 5 consists of a homogenous black to greenish-grey clayey silt/silt. Occasional faint laminae are preserved with sparse occurrences of the molluscs *Mulinia lateralis* and *Anomalocardia cuneimeris*. The facies also contains foraminifera and between 1 and 15% sand-sized material. Based on its location and characteristics, sedimentary facies 5 is interpreted as representing open-bay or distal upper-bay deposits.

Sedimentary facies 6: Sedimentary facies 6 consists of well-laminated greenish-grey clayey silt/silt with light grey to white laminae (Fig. 9). The light laminae are composed of carbonate minerals and rarely sand or shell hash. This facies also contains a few juvenile molluscs (*Anomalocardia cuneimeris*, *Chione cancellata* and *Mulinia lateralis*), as well as calcareous foraminifera. Based on its presence in cores from the modern open bay, this facies is interpreted as representing open-bay or back-spit lagoon deposits.

Spits. As the terrestrial input of sand is presently limited, a number of the beaches within Baffin Bay are composed of shell-hash material (Fig. 16). Modern beach and spit deposits comprise sedimentary facies 7.

Sedimentary facies 7: Sedimentary facies 7 consists of grey-tan shelly fine sand or shell hash (Fig. 16). The shell fragments are dominantly from the following mollusc species: *Mulinia lateralis*, *Anomalocardia cuneimeris*, *Chione cancellata*, *Nuculana acuta*, *Lucina multilineata* and

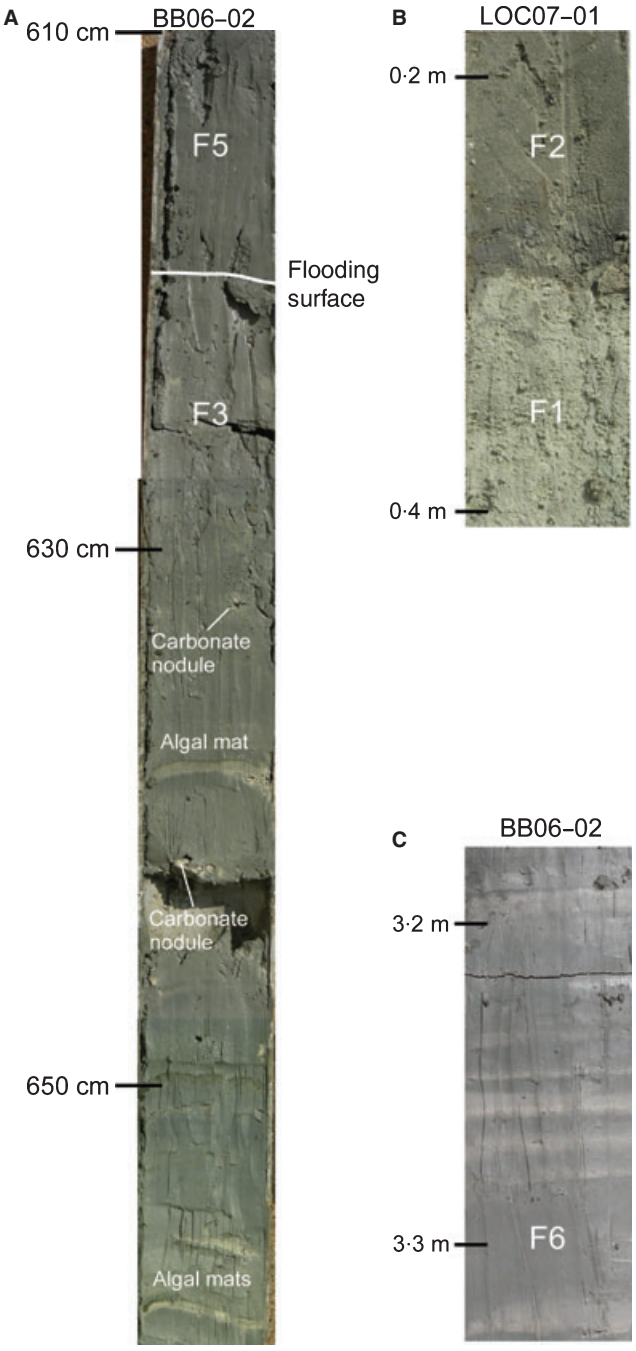

Fig. 9. Core photographs of select sedimentary facies from facies assemblage 1 representing the modern environments of Baffin Bay. (A) Sedimentary facies 5 representing open-bay deposits overlying sedimentary facies 3 representing mud-flat deposits. (B) Sedimentary facies 1 and 2 representing the modern fluvial floodplain and fluvial channel deposits, respectively. (C) Sedimentary facies 6 representing well-laminated open-bay deposits.

Retusa canaliculata. The shell fragments higher in the cores are almost exclusively *Anomalocardia cuneimeris*. Plant fragments are also found within the sandy shell hash/shelly sand.

Washover/lower bay. The lower reaches of Baffin Bay behind Padre Island contain an area of sandy washovers. Similar deposits are also found in the cores beneath the worm-tube reefs. These deposits comprise sedimentary facies 8.

Sedimentary facies 8: Sedimentary facies 8 consists of a grey very-fine to fine sand with occasional cross-bedding, laminations or mottling. The sands contain few to several shell fragments, including *Anomalocardia cuneimeris*, *Anadara* sp., *Neritina (Vitta) virginea* and *Meioceras nitidum*. The sands are clean, well-sorted and some of the sands are carbonate coated.

Serpulid worm-tube reefs. Originally mapped by J.P. Breuer, Rusnak (1960) and Andrews (1964) showed a map of the location of over 120 serpulid worm-tube reefs within Baffin Bay originally

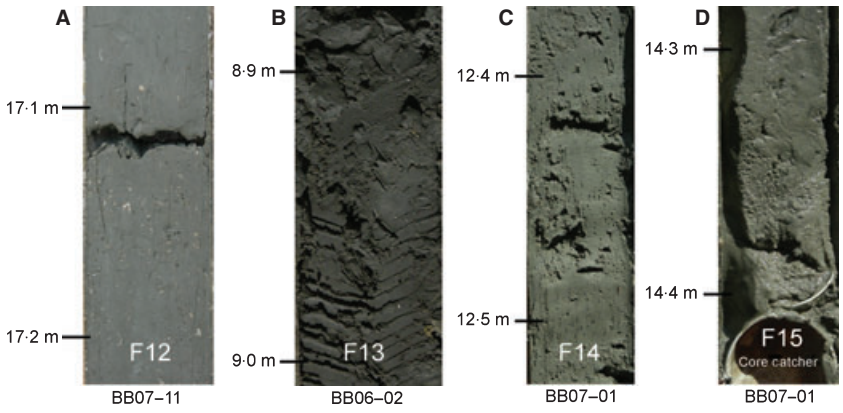

Fig. 10. Core photographs of the facies comprising facies assemblage 2. (A) Sedimentary facies 12 representing open-bay deposits from a less-arid time. (B) Sedimentary facies 13 representing floodplain deposits from a less-arid time. (C) Sedimentary facies 14 representing delta-plain deposits. (D) Sedimentary facies 15 representing mouth-bar or marine-influenced fluvial deposits.

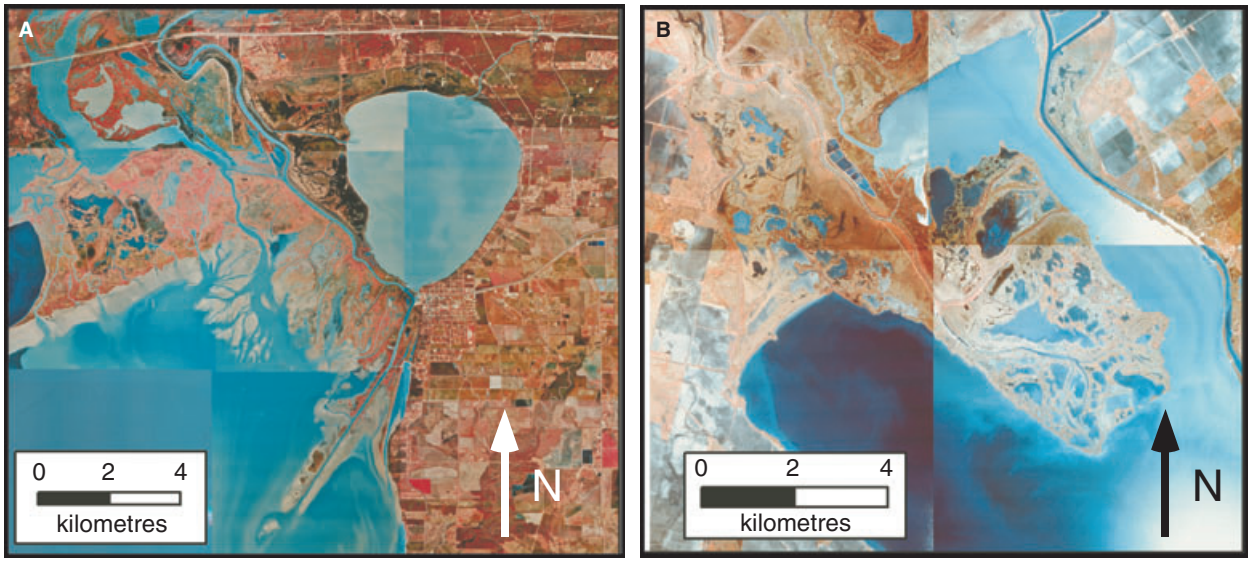

Fig. 11. Aerial photography of: (A) the Trinity bayhead delta in Galveston Bay, Texas; and (B) the Guadalupe Delta in San Antonio Bay, Texas. See Fig. 1 for bay locations. Aerial photographs courtesy of the Texas Natural Resources Information System (http://www.tnris.state.tx.us).

created by J. P. Breuer (Fig. 2). The reefs appear to fill the same ecological niches as oyster reefs in other estuaries. The reefs occur in water depths between 0·5 and 2·5 m and extend 8 to 15 cm above mean sea-level and up to 40 cm above mean sea-level during the lowest tides (Andrews, 1964). They occur mostly along the margins of the bay and not in the bay centres.

In a detailed study of these reefs, Andrews (1964) identifies two major types of serpulid worm-tube reefs in Baffin Bay and Laguna Madre. The first type of reef is a patch reef, which is a small isolated reef between 5 and 10 m in diameter and elongate perpendicular to the prevailing wind direction (Andrews, 1964; Glumac *et al.*, 2004). The second type of reef is reef, which are broad areas covered with scattered reef rocks. Andrews (1964) also identifies two types of fabric to the reef structure: random growth and oriented growth. The random growth reef rocks consist of worm-tubes that grew in random orientations. The oriented growth reef rocks consist of worm-tubes aligned parallel to one another (Fig. 17). Andrews (1964) suggests that the random fabric to the reef rock represents times of poor environmental conditions, while the oriented fabric represents growth of the reefs during optimal environmental conditions. Glumac *et al.* (2004) analysed oxygen and carbon isotopes from the random and oriented tubes and found that the random tubes had a larger range of isotope values, while the oriented tubes had less variability in isotope values. Glumac *et al.* (2004) suggested that the greater variability in isotope values indicated that the random worm-tubes grew during time periods of rapidly changing water temperature, salinity, and organic productivity within Baffin Bay.

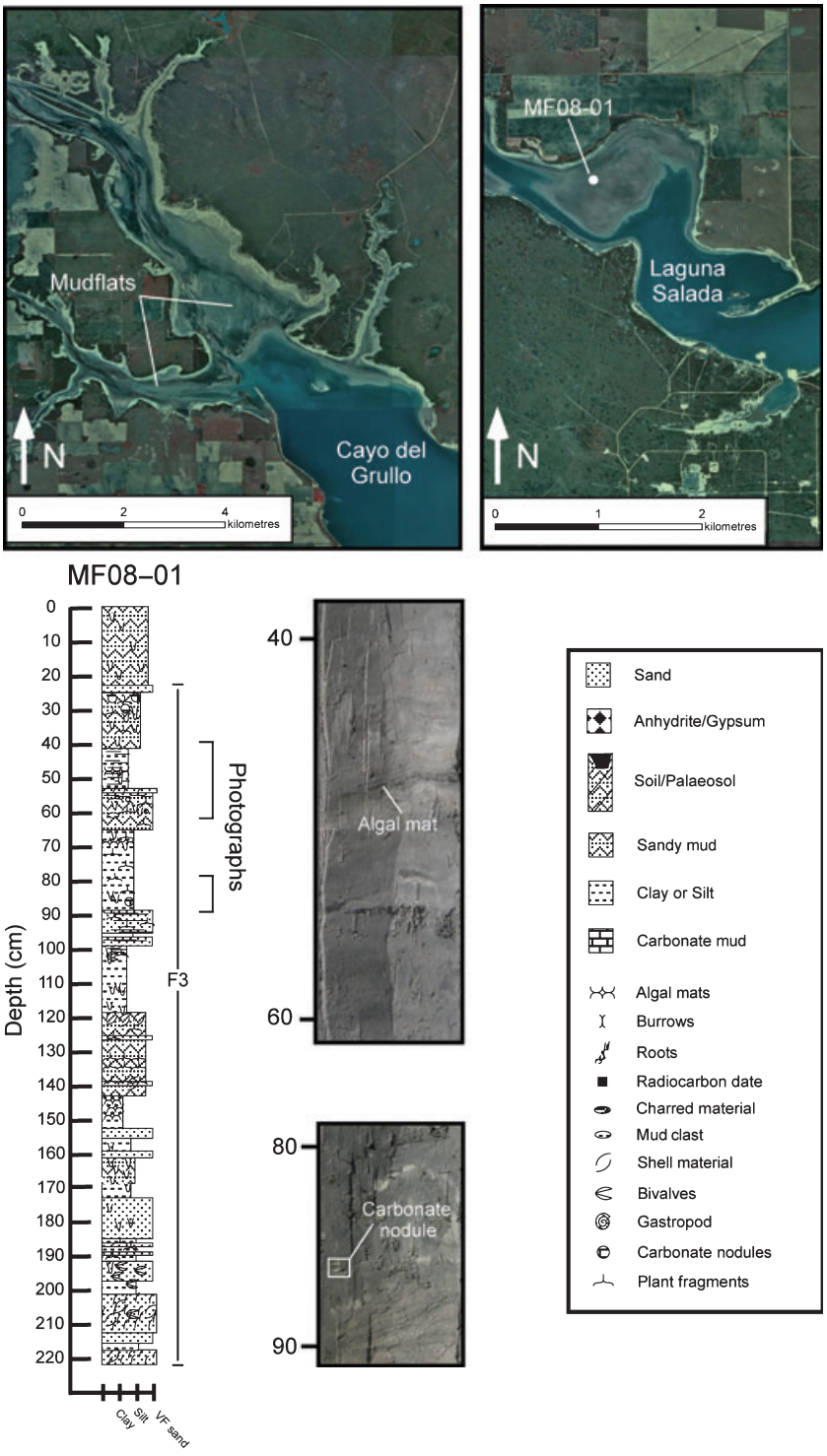

Fig. 12. Aerial photographs, core description and core photograph of the mud-flats in the upper reaches of the Baffin Bay tributary bays. See Fig. 1 for general location.

A series of cores was obtained along a transect orientated radially away from one of the lower Baffin Bay reefs (Fig. 18). The reef sampled appears to have grown on top of a sandy substrate (facies 8), which is consistent with the observations of Andrews (1964) who found that they always existed in areas of sandy or muddy-sand substrates. Two major facies are identified above facies 8 within these cores.

Sedimentary facies 9: In the two cores closest to the reef, a thin but distinctive facies about 10 cm thick (facies 9, Table 2) is found between the sandy interpreted substrate (facies 8) and another facies consisting of alternating sandy shell hash,

Fig. 13. Photographs of the algal mats covering the mud-flats in the upper reaches of Baffin Bay. (A) Mud flats during low wind tide. (B) Mud flats inundated by high wind tide. (C) Algal mats during low wind tide. (D) Algal mats during high wind tide. Persons for scale are *ca* 1·8 m tall.

shelly sand and sandy silt (facies 10, Table 2). Sedimentary facies 9 consists of grey fine sands with an occasional brown sand lamina and laminae of plant material (Fig. 18). It contains the gastropods *Neritina virginea* and *Cerithium* sp., both indicative of shallow grassy areas (Andrews, 1971), and an abundance of other shell and plant fragments with some worm-tube fragments. The sand grains are both calcareous as well as carbonate-coated quartz grains. This facies represents the grass flats around the serpulid reefs.

Sedimentary facies 10: Sedimentary facies 10 contains a tan-grey bedded sand with alternating fine sandy shell hash and shelly fine sand with sand silt laminae (Fig. 18). It is usually found above facies 9. Facies 10 is dominated by bivalve fragments and contains few worm-tube fragments. Andrews (1964) made a similar observation that, with the exception of the debris immediately windward of the reef (<25 feet), on average less than 5% of the coarse fraction (>63 μm) is composed of worm-tube debris. The scarcity of worm-tube debris testifies to the resilience of the reefs in their present wave climate. The shell fragments are dominantly *Mulinia lateralis*, *Brachidontes* sp. and *Anomalocardia cuneimeris*. The sand grains are carbonate-coated quartz or carbonate grains. This facies represents the distal worm-tube reef facies.

Barrier island sands. Although not sampled specifically for this study, the barrier-island deposits of Padre Island have been well-studied by others (Fisk, 1959). The bases of several cores in lower Baffin Bay sample a clean greenish-grey very fine sand with faint laminations and *in situ* carbonate nodules. These deposits are well-sorted and composed almost exclusively of quartz. No shell fragments, plant fragments, ostracods or foraminifera were found within this facies. This facies (facies 11) is interpreted to represent some type of barrier-island deposit (for example, beach,

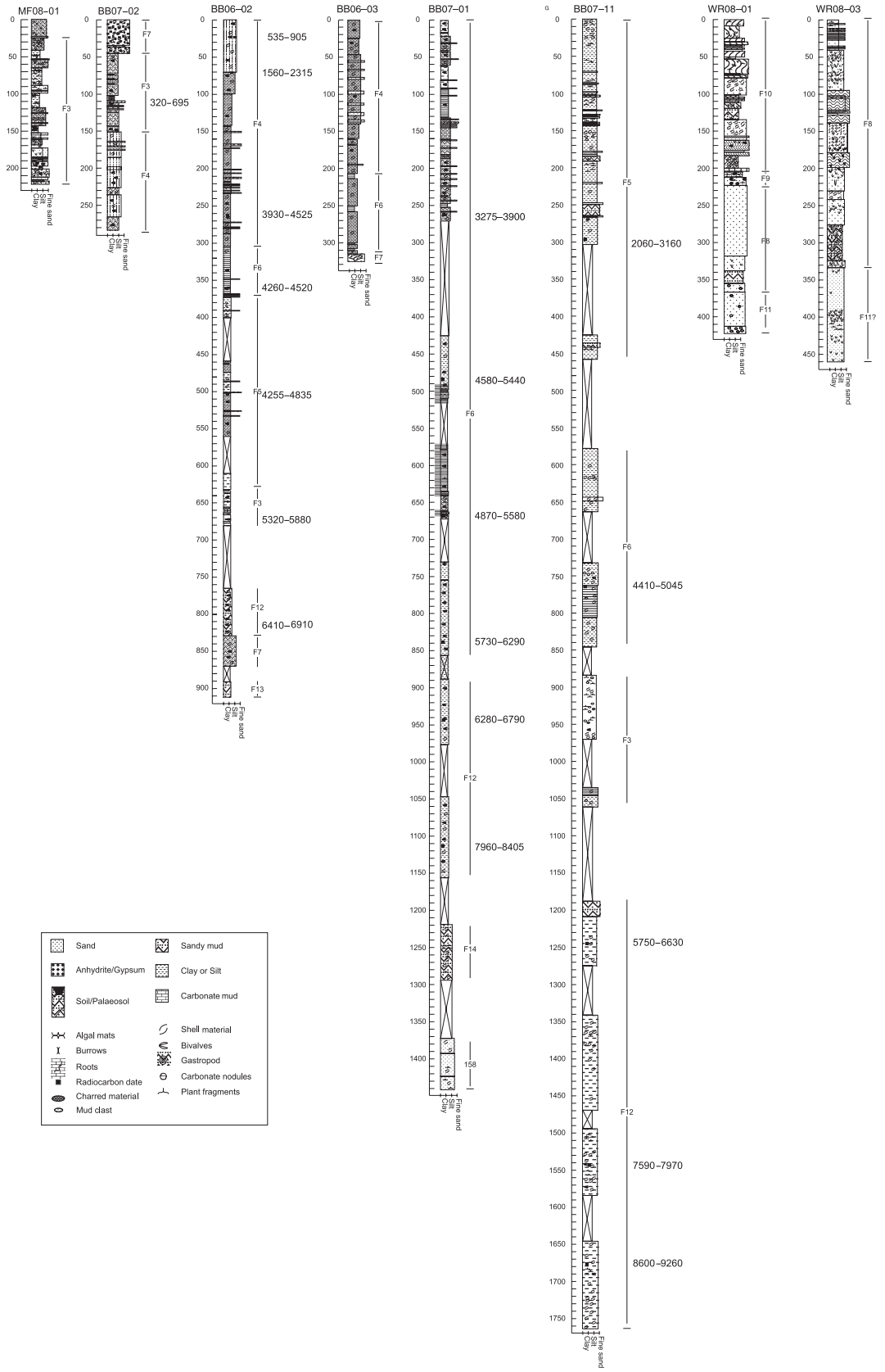

Fig. 14. Core descriptions used to make the generalized dip profile of depositional environments through Baffin Bay. See Fig. 1 for core locations. All ages are in calendar years BP.

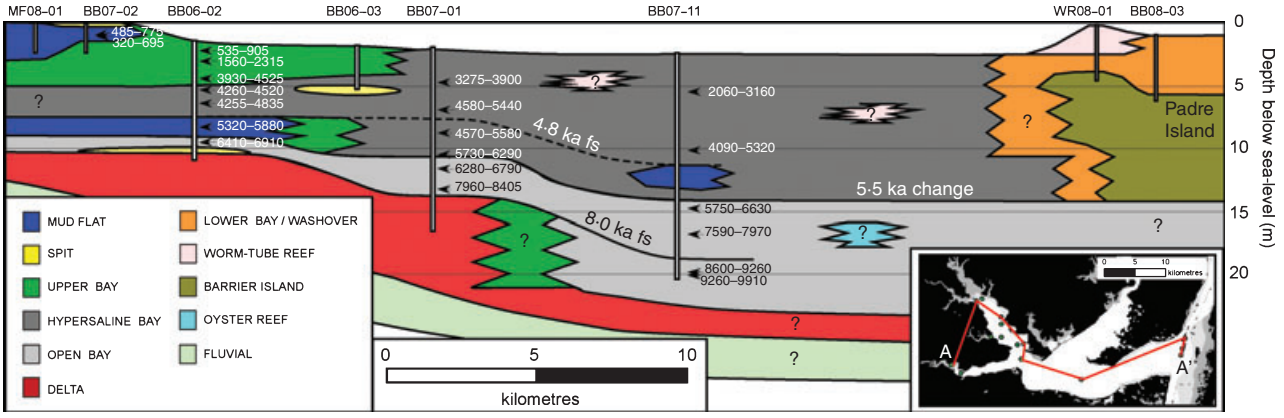

Fig. 15. Dip profile of depositional environments in Baffin Bay. See Fig. 14 for core descriptions. fs, flooding surface.

aeolian or wind flat). As beach, aeolian and wind-flat deposits are very difficult to distinguish within cores, no distinction is made as part of this study.

Ooids. Although not sampled in this study, ooids are found along the shallow shorelines of Baffin Bay (Fig. 2); their occurrence is limited largely to the northern shores of Baffin Bay and they are most common around Kleberg Point (Land *et al.*, 1979; Fig. 2). Other notable concentrations of ooids are found at the mouth of Baffin Bay and just to the north of the mouth of Baffin Bay in Laguna Madre (Rusnak, 1960; Freeman, 1962). Post-bomb concentrations of ^{14}C within the outside layers of the ooids indicate that they are forming today (Land *et al.*, 1979). Rusnak (1960) noted that their frequency decreases with distance from the shore, consistent with wave-agitation as a requirement for their formation. In addition, Freeman (1962) noted a decrease in symmetry and polishing with decreasing energy conditions.

Three types of coatings have been identified within the ooids of Baffin Bay: tangential (concentric), micritic (aggregate or random) and radial (Rusnak, 1960; Freeman, 1962; Dalrymple, 1964; Land *et al.*, 1979). The oolitic coatings are composed of two major carbonate minerals: aragonite and Mg-calcite (Land *et al.*, 1979). Aragonite is the most common mineral, but most radial coatings are composed of Mg-calcite (Land *et al.*, 1979). The type of coating appears to be controlled by the amount of wave agitation or possibly the amount of environmental organic acids rather than the Mg/Ca ratios of the waters or the mineralogy of the substrate (Land *et al.*, 1979). In addition, Land *et al.* (1979) found no conclusive evidence that the oolitic coatings were controlled by algal activity, as some have suggested.

Facies assemblage 2

In addition to the facies found in the modern environments of Baffin Bay, four facies were found within the cores that have no modern analogues within Baffin Bay but have similarities to modern environments in other Gulf of Mexico estuaries further to the north (Fig. 10). These were grouped into facies assemblage 2 and consist of sedimentary facies 12 to 15. Facies assemblage 2 is only found in the deeper portions of the incised-valley fill (Fig. 14).

Sedimentary facies 12. Sedimentary facies 12 is a light grey clayey silt/sandy silt (very fine sand) without any sedimentary structures (Fig. 10). What makes this unit different from other facies is the prevalence of shell material and the diversity of fauna represented by the shell material. Common molluscs within this facies include: *Mulinia lateralis*, *Retusa canaliculata*, *Macoma tenta*, *Chione cancellata*, *Crassostrea virginica* and *Nuculana acuta*. *Anomalocardia cuneimeris* is also occasionally found within this facies but does not dominate the fauna as it does in the estuarine units of facies assemblage 1. Based on the fauna, sedimentary structures, presence of foraminifera and association with seismic facies interpreted to represent oyster reefs, sedimentary facies 12 is interpreted as deposits from an open-bay environment from a wetter time or a time when the bay was not as isolated from the Gulf of Mexico.

Sedimentary facies 13. Sedimentary facies 13 is a stiff, dark bluish-grey sandy clay with plant fragments (Fig. 10). Based on the absence of shell material and foraminifera as well as its grain size and presence of plant fragments, this unit is interpreted to represent a fluvial floodplain environment.

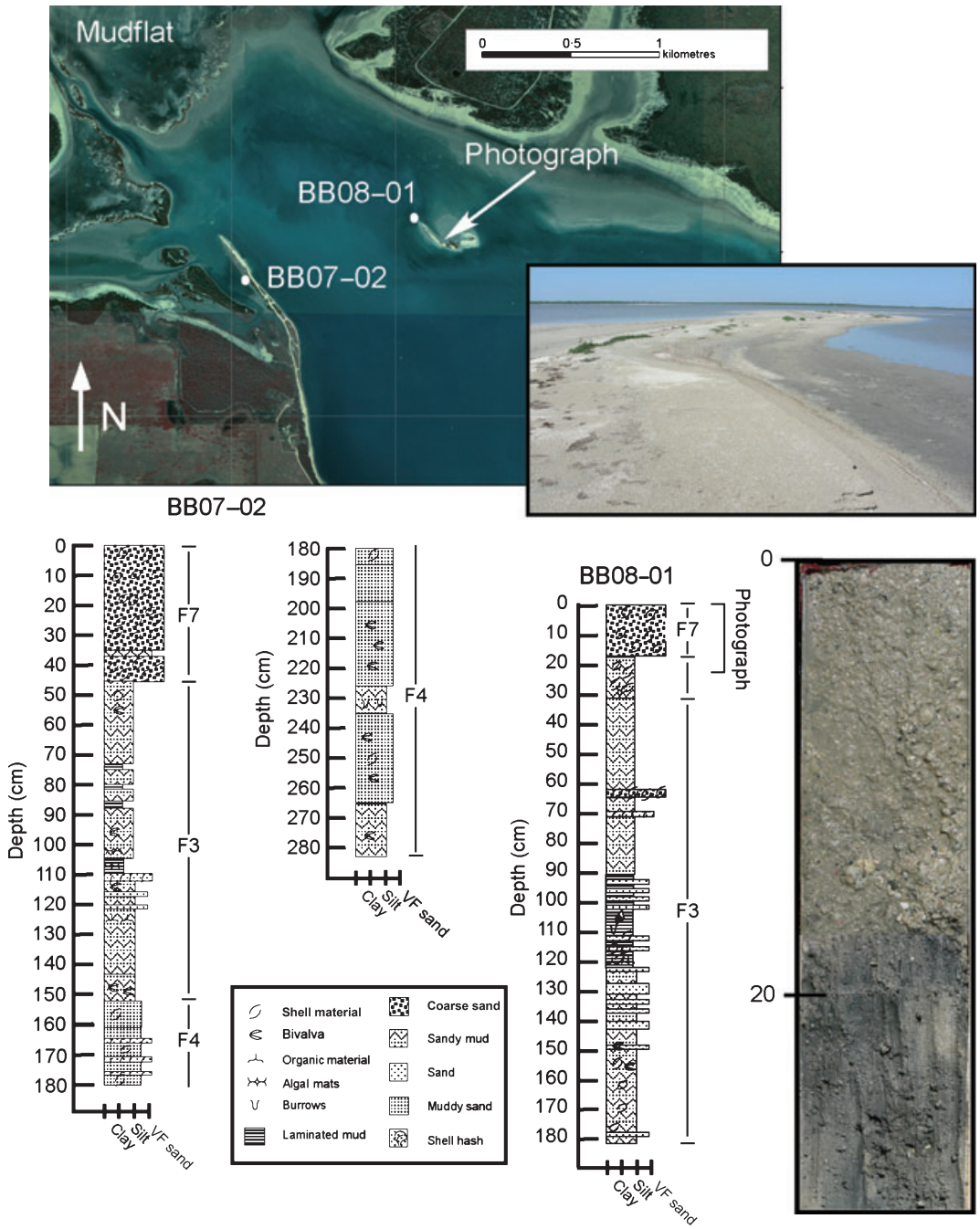

Fig. 16. Aerial photograph, core photograph and core descriptions through a modern spit and 'internal' barrier island. See Fig. 1 for general location.

Sedimentary facies 14. Sedimentary facies 14 is a dark greenish-grey sandy (very fine sand) mud with root casts, alternating mud sand laminae and lots of plant fragments (Fig. 10). It also contains the molluscs *Turbonilla* sp., *Chione cancellata* and *Retusa canaliculata*. Based on the root casts, fauna and presence of plant fragments, this unit is interpreted to represent a bayhead-delta plain.

Sedimentary facies 15. Sedimentary facies 15 is a dark greenish-grey fine sand (>80% sand) with a few shell fragments, ostracods, calcareous and porcelaneous foraminifera and plant fragments (Fig. 10). The shell fragments are mostly pelecepods and are not large enough for positive identification. Seismic profiles through this facies are chaotic in nature (Fig. 6). Based on the presence of plant and shell fragments and its grain size, this

Fig. 17. Photograph of a section of worm-tube reef.

unit is interpreted to represent either a bayhead-delta mouthbar or the deposits from the seaward-most reaches of a fluvial channel.

Chronology

Samples from select mollusc shells and a few plant fragments and algal mats were analysed for ^{14}C age at the University of Tokyo and Beta Analytic, Inc. In all, 22 samples were dated according to the methodology of Yokoyama *et al.* (2000, 2006). A summary of the ^{14}C dates is given in Table 3. One important correction that needs to be made to ^{14}C dates when comparing with other geologically dated events is the selection of an appropriate radiocarbon reservoir. Simms *et al.* (2009) obtained a paired optically stimulated luminescence/^{14}C age from a shallow lagoon on the southern margins of Baffin Bay. Simms *et al.* found a reservoir correction of around 200 years best brought optically stimulated luminescence and ^{14}C ages into agreement. A reservoir of 200 years falls within the range of other reservoirs determined within the Gulf of Mexico (Aten, 1983). All ages in this study were corrected for $^{12}C/^{13}C$ and appropriate carbon reservoirs and calibrated using the northern hemisphere terrestrial curve (after application of local ^{14}C reservoir) of Calib 5.0 (Reimer *et al.*, 2004). This approach allows a comparison of the changes recorded within the fill of Baffin Bay with changes found in other studies throughout the Gulf of Mexico.

DISCUSSION

Holocene history

Facies assemblage 2 at the base of Baffin Bay is similar to the facies found in other estuaries of the north-western Gulf of Mexico (Shepard & Moore, 1960; McEwen, 1969; Anderson *et al.*, 2008; Maddox *et al.*, 2008; Simms *et al.*, 2008). The bases of cores BB07-01 and BB06-02 contain facies very similar to other bayhead deltas of the Texas estuaries (McEwen, 1969; Donaldson *et al.*, 1970; Simms *et al.*, 2008). For example, facies 15, which is interpreted as mouthbar deposits, is very similar to the delta-front deposits described from the modern Guadalupe and Trinity bayhead deltas further to the north along the Gulf of Mexico by Donaldson *et al.* (1970) and McEwen (1969), respectively. However, these facies (facies 13, 14 and 15; Table 2) are not found among the modern environments of Baffin Bay. The existence of a well-developed bayhead delta suggests that sediment supplied by the three creeks flowing into Baffin Bay was greater during the past than it is today. This difference suggests that some significant changes have occurred within the Baffin Bay system throughout the Late Pleistocene and Holocene.

Flooding surfaces or transgressive overlap boundaries (Fletcher *et al.*, 1993; Anderson *et al.*, 2001) are common within the fill of Quaternary systems; their causes can range from allocyclic controls such as sea-level rise or climate changes (Fletcher *et al.*, 1993; Simms *et al.*, 2008) or they can be related to local autocyclic processes such as the flooding of terraces (Rodriguez *et al.*, 2005). Within the fill of Baffin Bay (Texas) two, or possibly three, distinct periods of large-scale changes are identified. Two of these changes are associated with flooding surfaces and one of these changes is marked by a change in the character of the fill. The flooding surfaces are identified as prominent widespread continuous seismic reflections between seismic facies (Fig. 6) as well as abrupt sedimentary contacts within cores (Fig. 9).

The older of the two flooding surfaces occurred around 8 ka. The age of the flooding surface is constrained by its position between 8600 to 9260 cal years and 7590 to 7970 cal years in core BB07-11 and immediately below 7960 to 8405 cal years in core BB07-01. This event is marked by a

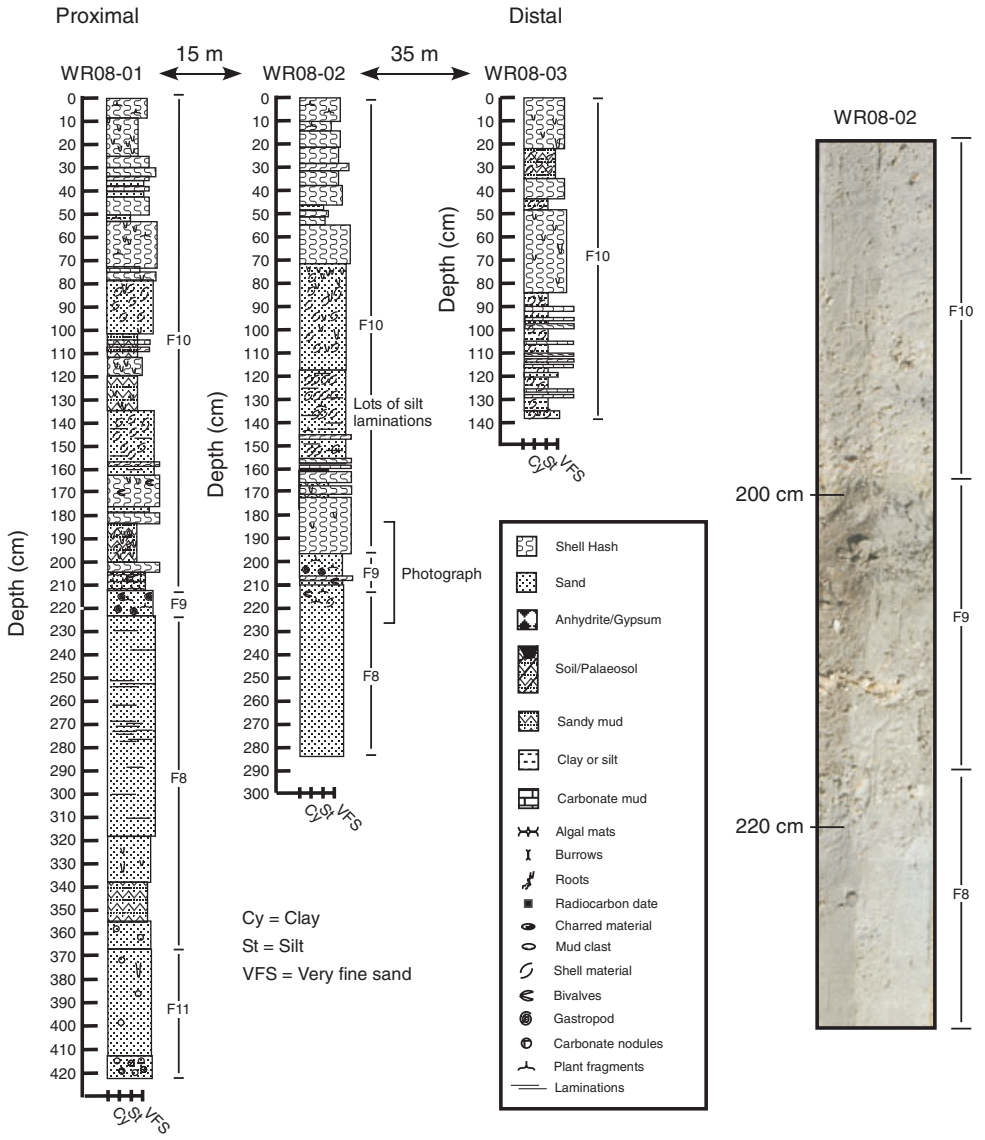

Fig. 18. Core descriptions and photograph of cores taken near a worm-tube reef. See Fig. 1 for core locations.

backstepping of the bayhead delta by >15 km as it backsteps to a location landward of the seismic survey (Fig. 8). This surface is marked by a widespread continuous prominent reflection in seismic profiles (Fig. 6), but is located between core breaks in the two cores that sample to its depth (cores BB06-02 and BB07-01). The one core that does sample a complete section through this contact is in a location seaward of the bayhead delta in which open-bay deposits overlie open-bay deposits; hence, no core constrains the abruptness of the boundary in sedimentary section. However, it is marked by a high amplitude continuous seismic reflection (Fig. 6) suggesting a strong impedance contrast consistent with an abrupt sedimentary contact. Maps illustrating the environments above and below the flooding surface, largely constructed using seismic facies, show a large change in the structure of the bay (Fig. 8). A similar event is found within many other estuaries across the Gulf of Mexico (Simms *et al.*, 2008; Anderson *et al.*, 2008; Milliken *et al.*, 2008b,c; Rodriguez *et al.*, 2008) and the world (Hori & Saito, 2007; Cronin *et al.*, 2007). Its timing roughly corresponds to the 8·2 ka climatic event recorded in the Greenland Ice Cores (Alley *et al.*, 1997) which, depending on location, also resulted in a relative sea-level rise of 0·5 to 1 m (Kendall *et al.*, 2008). This flooding surface is interpreted as the result of the sea-level rise associated with this climate event.

The second period of large-scale change to Baffin Bay occurred around 5·5 ka and is marked by a change in sedimentary facies through most of

Table 3. ^{14}C ages collected during this study.

Lab	Lab code	Sample	Material	^{14}C age *	Error	$d^{13}C$	$d^{13}C$ and reservoir corrected†	Error‡	Calendar age§
University of Tokyo	MTC-12307	BB07-11 298	*Anomalocardia cuneimeris*	2305	190	1·07¶	2530	215	3160–2060
University of Tokyo	MTC-12308	BB07-11 765	*Anomalocardia cuneimeris*	3955	65	1·07¶	4180	120	5045–4410
University of Tokyo	MTC-12309	BB07-11 1245	Frag – Tagelis sp.**	5215	155	−0·33††	5420	185	6630–5750
University of Tokyo	MTC-12310	BB07-11 1543	*Mulinia lateralis*‡‡	6760	60	−0·82**	6950	115	7970–7590
University of Tokyo	MTC-12311	BB07-11 1690	*Mulinia lateralis*‡‡	7840	60	−0·82**	8030	115	9260–8600
University of Tokyo	MTC-12312	BB07-11 1727	Unknown	8340	70	−0·33††	8540	120	9910–9260
University of Tokyo	MTC-08627	BB06-02 22-25	*Callocardia/Agripoma texasina*‡‡	530	30	−0·33††	730	105	905–535
University of Tokyo	MTC-08628	BB06-02 70	*Rangia flexuosa* (J) ‡‡	1760	120	−0·33††	1960	160	2315–1560
University of Tokyo	MTC-09750	BB06-02 262	Anomalocardia cuneimeris‡‡	3615	35	1·07¶	3840	105	4525–3930
Beta Analytical	Beta-223689	BB06-02 359	Wood fragment	3950	40	−26·3	–	–	4520–4260
University of Tokyo	MTC-08029	BB06-02 502	Anomalocardia cuneimeris‡‡	3825	35	1·07¶	4050	105	4835–4255
Beta Analytical	Beta-227647	BB06-02 674	Algal mat	5040	40	−14·5	4840	105	5880–5320
University of Tokyo	MTC-09749	BB06-02 824	Nuculana acuta‡‡	5645	40	−0·33††	5850	105	6910–6410
Beta Analytical	Beta-227646	BB07-02 103-108	Algal mat	830	40	−10·7	630	105	775–485
Beta Analytical	Beta-227649	BB07-02 105	*Anomalocardia cuneimeris*‡‡	760	40	NR	560	105	695–320
University of Tokyo	MTC-09748	BB07-04 232	Unknown	2920	40	−0·33††	3120	105	3575–3005
University of Tokyo	MTC-08900	BB07-01 262	Unknown‡‡	3140	75	−0·33††	3340	125	3900–3275
University of Tokyo	MTC-08899	BB07-01 485	*Rangia flexuosa* (J) ‡‡	4170	80	−0·33††	4370	130	5440–4580
University of Tokyo	MTC-08904	BB07-01 667	*Anomalocardia cuneimeris*	4350	75	−0·33††	4550	125	5580–4870
University of Tokyo	MTC-08901	BB07-01 837	*Rangia flexuosa* (J) ‡‡	5050	80	1·07¶	5250	130	6290–5730
University of Tokyo	MTC-08903	BB07-01 946	*Mulinia lateralis*‡‡	5515	75	−0·82**	5710	125	6790–6280
University of Tokyo	MTC-08902	BB07-01 1113	*Mulinia lateralis*‡‡	7175	80	−0·82**	7370	130	8405–7960

*Ages from Beta Analytical corrected for actual $d^{13}C$ measured from sample.
†Using a reservoir correction of 200 years.
‡Based on summing the squares of measurement error and reservoir error variation (1/2 reservoir value).
§Based on northern hemisphere atmosphere curves of Calib 5.0.
¶Average $d^{13}C$ from *Anomalocardia cuneimeris* from south Texas (n = 3).
**Average $d^{13}C$ from *Mulinia lateralis* from south Texas (n = 12).
††Average $d^{13}C$ from mollusks of different species from south Texas (n = 49).
‡‡Articulated.

the incised-valley fill (Fig. 15). This change is more gradual than the changes associated with the 8 ka event. The timing of the event is constrained to be between 5730 to 6290 cal years and 6280 to 6790 cal years in core BB07-01, between 4090 to 5320 cal years and 5750 to 6630 cal years in core BB07-11, and between 5320 to 5880 cal years and 6410 to 6910 cal years in core BB06-02. Below this interval, facies 12 is found (Fig. 14, Table 2), a facies characterised by a much more diverse molluscan fauna. In addition, the laminated mud facies (facies 6) is only found in the shallower portions of the incised-valley fill (Fig. 14, Table 2). No carbonate muds or algal mats were sampled below this interval. At 5·5 ka the bay environments represented by facies assemblage 2 (for example, similar to other present Texas bays) change to those environments of its present, semi-arid character represented by facies assemblage 1. This event is close to the time that Padre Island formed (Fisk, 1959) and also during the time of the Altithermal or mid-Holocene drought throughout the central United States (Antevs, 1955; Dean *et al.*, 1996). Most climatic records from Texas show increased aridity during this time (Bryant & Holloway, 1985; Toomey *et al.*, 1993; Nordt *et al.*, 2002). The increase in aridity probably contributed to the decrease in sediment supplied by the creeks flowing into Baffin Bay as evidenced by the change from a fluvial-dominated bayhead delta to the modern mud-flats. The 5·5 ka event is interpreted as representing the isolation of Baffin Bay from the Gulf of Mexico by the formation of Padre Island, concurrent with a regional drying trend across the area. It is around 5·5 ka that the current sedimentary characteristics of the incised-valley fill were established.

A third event, a second possible flooding surface, was identified within Baffin Bay. This flooding surface is seen as a continuous and prominent reflection in seismic profiles (Fig. 6) and an abrupt contact in sedimentary facies in cores (Figs 9 and 15). In some cases, this event is marked by an erosional surface across the internal spits (Fig. 19). Within cores BB07-11 and BB06-02, it is marked by a change from facies 3 to facies 6 or 5, marking the flooding of mud-flats (Figs 9, 14 and 15). This

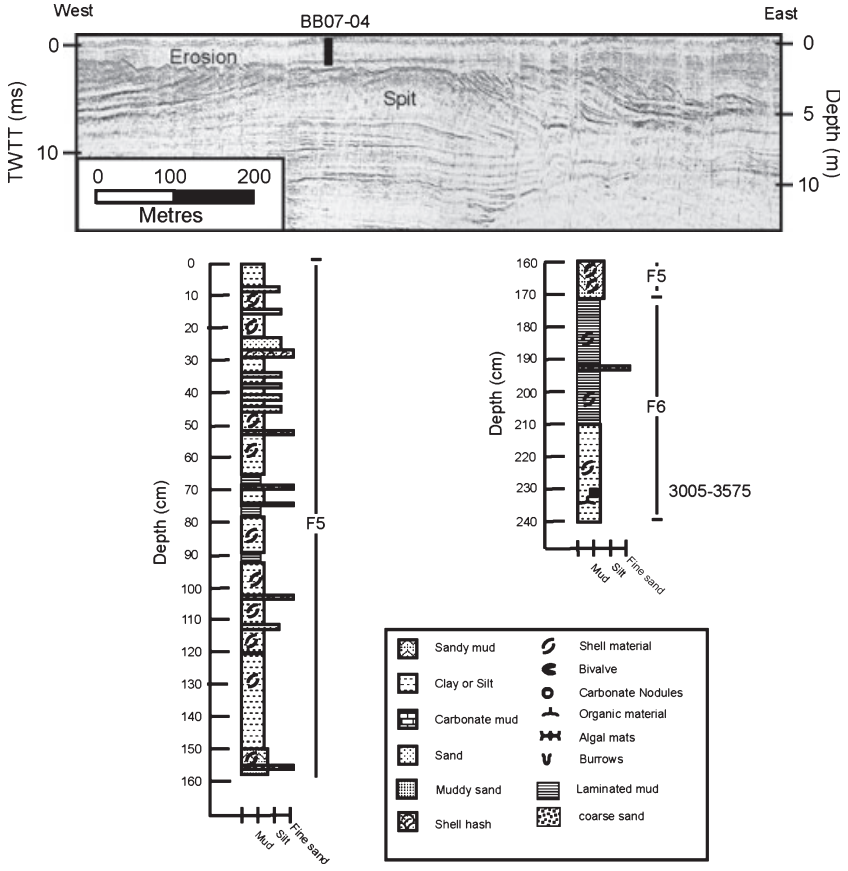

Fig. 19. Seismic profile through an interpreted spit truncated during the time of the formation of the 4·8 ka flooding surface. Also shown is a description of core BB07-04, which places some constraint on the age of the surface in this location. See Fig. 8 for general location. All ages are in calendar years BP. TWTT, two-way travel time.

backstepping event does not appear to be as extensive as the two earlier events. However, the full scale of this final backstepping event could not be determined because the extremely shallow water prevented the seismic survey from extending into the upper reaches of Baffin Bay. Available age constraints suggest that this event occurred around 4·8 ka. The event occurred between 4255 to 4835 cal years and 5320 to 5880 cal years in core BB06-02, between 4870 to 5580 cal years and 4580 to 5440 cal years in core BB07-01, and between 5750 to 6630 cal years and 4090 to 5320 cal years in core BB07-11 (Figs 14 and 15). Some time after 4·0 ka, the mud-flats of Baffin Bay appear to prograde seaward (Fig. 15). The bayhead deltas of several other Gulf of Mexico estuaries show a similar progradation in the Late Holocene suggesting a regional cause (Shepard & Moore, 1960; Anderson *et al.*, 2008; Simms *et al.*, 2008).

Criteria for recognising semi-arid and arid incised-valley fill within the rock record

Facies assemblage 1 can be used to gain some insights about the deposits found within incised valleys that filled during time periods marked by semi-arid and arid climates. Feldman *et al.* (2005) summarised the differences among incised valleys formed in wet and dry climates based on eight cyclothems in the Pennsylvanian of the mid-continent USA. These authors found that incised valleys formed during dry climates were generally smaller in dimension (both depth of incision as well as width) than those formed in wet climates. In a study of Miocene shelf deposits of the Eastern Mediterranean, Buchbinder & Zilberman (1997) found only minor amounts of incision associated with incised valleys during the Messinian desiccation event in an arid setting. Although the Baffin Bay incised valley is smaller than other incised valleys from the more humid Gulf of Mexico further to the east (e.g. Trinity – Thomas & Anderson, 1994; Brazos – Abdulah *et al.*, 2004), other variables may explain the smaller size of Baffin Bay. A study by Mattheus *et al.* (2007) suggests that the size of the drainage basin is more important than climate in determining the cross-sectional dimensions of incised valleys. The Rio Grande incised valley (Banfield & Anderson, 2004) located about 140 km to the south of Baffin Bay is much larger than the Baffin Bay incised valley, yet in a slightly drier climate. However, the climate setting of Baffin Bay has changed considerably through the last 120 kyr and has not always been semi-arid. Musgrove *et al.* (2001) suggested wetter climates for Texas throughout much of the fall in sea-level between 70 and 20 ka based on increased growth rates of speleothems from caves in central Texas. Based on the pollen and fauna of deposits from central Texas, Bryant (1977) and Toomey *et al.* (1993) suggest that the Last Glacial Maximum was wetter than present (Bryant, 1977; Toomey *et al.*, 1993). Feldman *et al.* (2005) do suggest that other factors could be contributing to the differences between the dimensions of incised valleys from the dry and wet cyclothems such as the character of the substrate. Thus, more work needs to be performed to determine whether drier climates result in smaller incised valleys.

Nevertheless, some of the other observations of Feldman *et al.* (2005) are in agreement with observations from Baffin Bay. In particular, Feldman *et al.* (2005) noticed a scarcity of coal within incised valleys from dry climates. Unlike other estuaries further to the east in the Gulf of Mexico (e.g. Galveston Bay – Anderson *et al.*, 2008; Lake Calcasieu – Milliken *et al.*, 2008b; Sabine Lake – Milliken *et al.*, 2008c) or along the Atlantic Coast of the USA (e.g. Chesapeake Bay – Nichols *et al.*, 1991), the upper bay and bay margins of Baffin Bay are devoid of significant peat deposits.

Based on facies assemblage 1 from Baffin Bay, several additional criteria can be used to identify semi-arid or arid conditions within the fill of incised valleys. The first is a fauna characteristic of hypersaline conditions. Baffin Bay contains two such examples. One example is the molluscs which, in the earlier deposits from Baffin Bay, interpreted as representing more mesic conditions, were more diverse including the presence of *Crassostrea virginica* (oysters), *Retusa canaliculata* and *Chione cancellata*. Breuer (1957) reports oyster mittens created by Native Americans suggesting wetter climates or better connection with the open Gulf of Mexico some time during the past. However, today the bay is dominated by two bivalves: *Anomalocardia cuneimeris* and *Mulinia lateralis* (Breuer, 1957). This change to a low-diversity fauna occurred around 5·5 ka. The second example of fauna characteristic of hypersaline conditions from Baffin Bay is the serpulid worm-tube reefs. Today, serpulids are not the dominant reef builders on a global scale; they only produce reefs in environments such as the hypersaline Baffin Bay or other hypersaline locations such as palaeo Lago Enrichquillo in the Dominican Republic (Glumac *et al.*, 2004).

Another criterion is the presence of aeolian deposits within the fill. Although not cored in

this study, one of the southern tributary valleys of the Baffin Bay System is choked with aeolian dunes that have migrated into the valley (Fig. 20). Along the West Sardinia coastline, Andreucci *et al.* (2006) identified a series of marine isotope stage 4 (MIS4, *ca* 60 to 70 ka) incised valleys filled predominantly with coarse braided stream, colluvial and aeolian deposits in an interpreted semi-arid setting. Similarly, in a study of the Upper Guadalupian (Late Permian) Yates Formation, Johnson (1997) identified a series of low-stand incised valleys filled with fluvial and aeolian deposits in an overall arid climate of the Permian Basin of west Texas.

The hypersaline environment of Baffin Bay favours the precipitation of carbonate mud and, in a few instances, evaporites (e.g. a large gypsum crystal recovered in core BB08-01); these may also be a key in recognising incised valleys that form in semi-arid and arid environments. However, carbonates and gypsum alone cannot be used as recognition of semi-arid or arid environmental conditions. In the north-eastern Gulf of Mexico along the Florida coast, carbonates form alongside siliciclastic systems in a humid climate (Wright *et al.*, 2005). Cann & Cronin (2004) identified a gypsum-bearing deposit in the Holocene Chesapeake Bay system that was forming not as the result of semi-arid or arid climates but from the influx and trapping of brine being produced from underlying Miocene rocks.

The characteristics of associated floodplain deposits also add insight into the climate setting of an incised valley. The fluvial floodplain deposits before and after a shift to more arid conditions within the Baffin Bay system are very different. The base of core BB06-02 contains a very dark, organic-rich floodplain deposit. On the other hand, core LOC07-01, recovered from the modern floodplain, is very organic poor and has an abundance of carbonate in the form of nodules; this results in a very different colour and lower total organic carbon values within the floodplain fluvial or deltaic deposits of this semi-arid system.

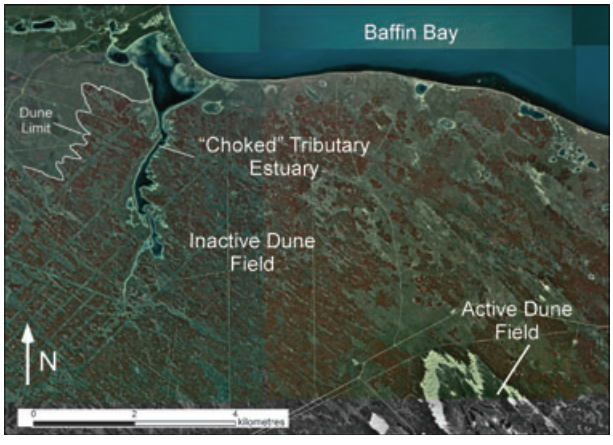

Fig. 20. Aerial photograph of the southern Baffin Bay tributary choked in aeolian dunes. Note the locations of relict dunes and active dunes. See Fig. 1 for general location.

CONCLUSIONS

Baffin Bay, Texas, is the flooded Last Glacial Maximum incised valley of the Los Olmos, San Fernando and Petronila Creeks. The Bay contains a record of Holocene sedimentation over the last 10 kyr. Because of its semi-arid climate setting, strong springtime and summer winds, and isolation from the open Gulf of Mexico, several depositional environments have formed within it distinguishing its fill from other well-studied Late Quaternary/Holocene incised-valley successions. These unusual depositional environments include: (i) well-laminated interbedded siliciclastic and carbonate muds within its central basin; (ii) ooid beaches; (iii) shelly internal spits and barrier islands; (iv) serpulid worm-tube reefs; and (v) prograding mud-flats in its upper tributary arms. These unusual depositional environments formed around 5·5 ka. Prior to this time, the estuarine environments were similar to those of other incised valleys of the Gulf of Mexico and Atlantic coasts, including the development of a well-developed bayhead delta. The sedimentary fill of Baffin Bay also records a major backstepping event at 8·0 ka, probably correlative to the 8·2 ka event recorded in many climate proxies worldwide and marked by a small-order jump in sea-level.

Based on the deposits from Baffin Bay, five criteria were identified that can be used to recognise incised valleys that formed within a semi-arid or arid environment: (i) hypersaline-tolerant fauna; (ii) aeolian deposits; (iii) carbonate and/or evaporite deposits; (iv) the absence of peat or other organic-rich deposits in the upper-bay and bay-margin areas; and (v) poorly developed bayhead deltas.

ACKNOWLEDGEMENTS

The authors would like to thank John Anderson, Tim Phillips, Jess Malicoate, Matin Alari, Taylor Troiani and Tyler Treece for their assistance in the field. We would also like to thank SubSea

Technologies of Houston, Texas for allowing use of the seismic equipment. Anna Cruse helped with the geochemical analysis of the sediments and James Puckette and Jay Gregg assisted in X-Ray diffraction. We would also like to thank Chris Fielding and an anonymous reviewer as well as Associate Editor David Mallison for comments that greatly improved the manuscript. This work was made possible by the generosity of the donors to the Petroleum Research Fund of the American Chemical Society through grant number 44868-GB8. Partial support was also provided by KAKENHI (221674003, 19340158, 20300294) and Global Environmental Research Fund RF-081.

REFERENCES

Abdulah, K.C., Anderson, J.B., Snow, J.N. and **Holdford-Jack, L.** 2004. The Late Quaternary Brazos and Colorado Deltas, offshore Texas – their evolution and the factors that controlled their deposition. In: *Late Quaternary Stratigraphic Evolution of the Northern Gulf of Mexico Margin* (Eds J.B. Anderson and R.H. Fillon), *SEPM Spec. Publ.*, **79,** 237–270, Tulsa, OK.

Alaniz, R.T. and **Goodwin, R.H.** (1974) Recent sediments of a hypersaline estaurine bay. *Trans. Gulf Coast Assoc. Geol. Soc.*, **24,** 308–313.

Alexander, C.R., Nittrouer, C.A., DeMaster, D.J., Park, Y.-A. and **Park, S.-C.** (1991) Macrotidal mudflats of the southwestern Korean Coast: a model for interpretation of intertidal deposits. *J. Sed. Petrol.*, **61,** 805–824.

Allen, G.P. and **Posamentier, H.W.** (1993) Sequence stratigraphy and facies model of an incised valley fill: the Gironde Estuary, France. *J. Sed. Petrol.*, **63,** 378–391.

Alley, R.B., Mayewski, P.A., Sowers, T., Stuiver, M., Taylor, K.C. and **Clark, P.U.** (1997) Holocene climatic instability: a prominent, widespread event 8200 yr ago. *Geology*, **25,** 483–486.

Anderson, J.B., Rodriguez, A.B., Fletcher, C. and **Fitzgerald, D.M.** (2001) Researchers focus attention on coastal response to climate change. *EOS Trans. Am. Geophys. Union*, **82,** 513.

Anderson, J.B., Rodriguez, A.B., Abdulah, K.C., Fillon, R.H., Banfield, L.A., McKeown, H. and **Wellner, J.S.** 2004. Late Quaternary Stratigraphic evolution of the northern Gulf of Mexico margin: a synthesis. In: *Late Quaternary Stratigraphic Evolution of the Northern Gulf of Mexico Margin* (Eds J.B. Anderson and R.H. Fillon), *SEPM Spec. Publ.*, **79,** 1–24, Tulsa, OK.

Anderson, J.B., Rodriguez, A.B., Milliken, K.T. and **Taviani, M.** 2008. The Holocene evolution of the Gavleston estuary complex, Texas: evidence for rapid change in estuarine environments. In: *Response of Upper Gulf Coast Estuaries to Holocene Climate Change and Sea-Level Rise* (Eds J.B. Anderson and A.B. Rodriguez), *Geol. Soc. Am. Spec. Pap.*, **443,** 89–104, Boulder, CO.

Andreucci, S., Pascucci, V. and **Clemmensen, L.** (2006) Upper Pleistocene coastal deposits of West Sardinia: a record of sea-level and climate change. *GeoActa*, **5,** 79–96.

Andrews, P.B. 1964. Serpulid Reefs, Baffin Bay, Southeast Texas. In: *Depositional Environments South-Central Texas Coast* (Eds S.L. Perkins, J.T.J. Schultz, G.E. Butterfield, T.P.L.J. Dowell and W.R. Payne), *Gulf Coast Assoc. Geol. Soc. Field Trip Guidebook*, 102–120, Corpus Christi, Texas.

Andrews, J. 1971. *Sea Shells of the Texas Coast*. University of Texas Press, Austin, TX, 298 pp.

Antevs, E. (1955) Geologic-climatic dating in the west. *Am. Antiquity*, **20,** 317–335.

Anthony, E.J., Lucien, M.O. and **Lang, J.** (2002) Sedimentation in a fluvially infilling barrier-bound estuary on a wave-dominated, microtidal coast: Oueme River estuary, Benin, West Africa. *Sedimentology*, **49,** 1095–1112.

Ardies, G.W., Dalrymple, R.W. and **Zaitlin, B.A.** (2002) Controls on the geometry of incised valleys in the Basal Quartz Unit (Lower Cretaceous), western Canada sedimentary basin. *J. Sed. Res.*, **72,** 602–618.

Ashley, G.M. and **Sheridan, R.E.** 1994. Depositional model for valley fills on a passive continental margin. In: *Incised-Valley Systems: Origin and Sedimentary Sequences* (Eds R.W. Dalrymple, R. Boyd and B.A. Zaitlin), *SEPM Spec. Publ.*, **51,** 286–301, Tulsa, OK.

Aten, L.E. 1983. *Indians of the Upper Texas Coast*. Academic Press, New York, 370 pp.

Banfield, L.A. and **Anderson, J.B.** 2004. Late Quaternary evolution of the Rio Grande Delta. In: *Late Quaternary Stratigraphic Evolution of the Northern Gulf of Mexico Margin* (Eds J.B. Anderson and R.H. Fillon), *SEPM Spec. Publ.*, **79,** 289–306, Tulsa, OK.

Behrens, E.W. (1963) Buried Pleistocene river valleys in Aransas and Baffin Bays, Texas. *Publ. Inst. Mar. Sci.*, **9,** 7–18.

Behrens, E.W. (1966) Surface salinities for Baffin Bay and Laguna Madre, Texas. *Contrib. Mar. Sci.*, **11,** 168–173.

Behrens, E.W. (1974) Holocene sea level rise effect on the development of an estuarine carbonate depositional environment: Baffin Bay, Texas. *Mem. Inst. Geol. Bassin Aquitaine*, **7,** 337–341.

Behrens, E.W. and **Frishman, S.A.** (1971) Stable carbon isotopes in blue-green algal mats. *J. Geol.*, **79,** 94–100.

Behrens, E.W. and **Land, L.S.** (1972) Subtidal Holocene dolomite, Baffin Bay, Texas. *J. Sed. Petrol.*, **42,** 155–161.

Bernard, H.A. 1950. *Quaternary Geology of Southeast Texas*. Lousiana State University, Baton Rouge, LA, 165 pp.

Blum, M.D., Morton, R.A. and **Durbin, J.M.** (1995) ''Deweyville'' terraces and deposits of the Texas Coastal Plain. *Trans. Gulf Coast Assoc. Geol. Soc.*, **45,** 53–59.

Blum, M., Misner, T.J., Collins, E.S., Scott, D.B., Morton, R.A. and **Aslan, A.** (2001) Middle Holocene sea-level rise and highstand at +2m, Texas Gulf Coast. *J. Sed. Res.*, **71,** 581–588.

Bowen, D.W. and **Weimer, P.** (2003) Regional sequence stratigraphic setting and reservoir geology of Morrow incised-valley sandstones (Lower Pennsylvanian), eastern Colorado and western Kansas. *AAPG Bull.*, **87,** 781–815.

Boyd, R., Dalrymple, R.W. and **Zaitlin, B.A.** 2006. Estuarine and Incised-Valley Facies Models. In: *Facies Models Revisited* (Eds H.W. Posamentier and R.G. Walker), *SEPM Spec. Publ.*, **84,** 175–235, Tulsa, OK.

Breuer, J.P. (1957) An ecological survey of Baffin and Alazan Bays, Texas. *Publ. Inst. Mar. Sci.*, **4,** 134–155.

Bryant, V.M. (1977) A 16,000 year pollen record of vegetation change in central Texas. *Palynology*, **1,** 143–156.

Bryant, V.M. and **Holloway, R.W.** (1985) The late Quaternary paleoenvironmental record of Texas. In: *Pollen Records of Late-Quaternary North American Sediments* (Eds V.M. Bryant and R.W. Holloway), pp. 39–70. American Association of Stratigraphic Palynologists Foundation, Dallas, TX.

Buchbinder, B. and **Zilberman, E.** (1997) Sequence stratigraphy of Miocene–Pliocene carbonate–siliciclastic shelf deposits in the eastern Mediterranean margin (Israel): effects of eustasy and tectonics. *Sed. Geol.*, **112,** 7–32.

Cann, J. and **Cronin, T.** (2004) An association of benthic foraminifera and gypsum in Holocene sediments of estuarine Chesapeake Bay, USA. *Holocene*, **14,** 614–620.

Coleman, J.M. and **Wright, L.D.** (1978) Sedimentation in an arid macrotidal alluvial river system: Ord River, Western Australia. *J. Geol.*, **86,** 621–642.

Cronin, T.M., Vogt, P.R., Willard, D.A., Thunell, R., Halka, J., Berke, M. and **Pohlman, J.** (2007) Rapid sea level rise and ice sheet response to 8,200-year climate event. *Geophys. Res. Lett.*, **34,** L20603.

Curray, J.R. (1960) Sediments and history of Holocene transgression, continental shelf, northwestern Gulf of Mexico. In: *Recent Sediments, Northwestern Gulf of Mexico* (Eds F.P. Shepard, F.B. Phleger and T.H.v. Andel), pp. 221–266. American Association of Petroleum Geologists, Tulsa, OK.

Dabrio, C.J., Zazo, C., Goy, J.L., Sierro, F.J., Borja, F., Lario, J., Gonzalez, J.A. and **Flores, J.A.** (2000) Depositional history of estuarine infill during the last postglacial transgression (Gulf of Cadiz, Southern Spain). *Mar. Geol.*, **162,** 381–404.

Dalrymple, D.W. (1964) *Recent Sedimentary Facies of Baffin Bay, Texas*. Rice University, Houston, TX.

Dalrymple, R.W., Zaitlin, B.A. and **Boyd, R.** (1992) Estuarine facies models: conceptual basis and stratigraphic implications. *J. Sed. Petrol.*, **62,** 1130–1146.

Dean, W.E., Ahlbrandt, T.S., Anderson, R.Y. and **Bradbury, J.P.** (1996) Regional aridity in North America during the middle Holocene. *Holocene*, **6,** 145–155.

Donaldson, A.C., Martin, R.H. and **Kanes, W.H.** 1970. Holocene Guadalupe Delta of Texas Gulf Coast. In: *Deltaic Sedimentation Modern and Ancient* (Ed. J.P. Morgan), *SEPM Spec. Publ.*, **15,** pp. 107–137.

Driese, S.G., Nordt, L.C., Lynn, W.C., Stiles, C.A., Mora, C.I. and **Wilding, L.P.** (2005) Distinguishing climate in the soil record using chemical trends in a vertisol climosequence from the Texas coast praire, and application to interpreting Paleozoic paleosols in the Appalachian Basin, U.S.A. *J. Sed. Res.*, **75,** 339–349.

Durbin, J.M., Blum, M. and **Price, D.M.** (1997) Late Pleistocene stratigraphy of the lower Nueces River, Corpus Christi, Texas: Glacio-eustatic influences on valley-fill architecture. *Trans. Gulf Coast Assoc. Geol. Soc.*, **47,** 119–129.

Eckles, B.J., Fassell, M.L. and **Anderson, J.B.** (2004) Late Quaternary evolution of the wave-storm-dominated central Texas shelf. In: *Late Quaternary Stratigraphic Evolution of the Northern Gulf of Mexico Margin* (Eds J.B. Anderson and R.H. Fillon), *SEPM Spec. Publ.*, **79,** 271–287, Tulsa, OK.

Elsner, J.B. and **Kara, A.B.** 1999. *Hurricanes of the North Atlantic: Climate and Society*. Oxford University Press, New York, 488 pp.

Feldman, H.R., Gibling, M.R., Archer, A.W., Wightman, W.G. and **Lanier, W.P.** (1995) Stratigraphic architecture of the Tonganoxie paleovalley fill (Lower Virgilian) in northeastern Kansas. *AAPG Bull.*, **79,** 1019–1043.

Feldman, H.R., Franseen, E.K., Joeckel, R.M. and **Heckel, P.H.** (2005) Impact of longer-term modest climate shifts on architecture of high-frequency sequences (Cyclothems), Pennsylvanian of midcontinent U.S.A. *J. Sed. Res.*, **75,** 350–368.

Fisk, H.N. (1959) Padre Island and the Laguna Madre Flats coastal south Texas. In: *2nd Coastal Geography Confer* (Ed. R.J. Russell), pp. 103–151. Office of Naval Research, Washington, DC.

Fletcher, C.H., Van Pelt, J.E., Brush, G.S. and **Sherman, J.** (1993) Tidal wetland record of Holocene sea-level movements and climate history. *Palaeogeogr. Palaeoclimatol. Palaeoecol.*, **102,** 177–213.

Freeman, T. (1962) Quiet water oolites from Laguna Madre, Texas. *J. Sed. Petrol.*, **32,** 475–483.

Garrison, J.R.J. and **Van den Bergh, T.C.V.** 2006. Effects of sedimentation rate, rate of relative rise in sea level, and duration of sea-level cycle on the filling of incised valleys: examples of filled and ''overfilled'' incised valleys from the upper Ferron Sandstone, Last Chance Delta, east-central Utah, U.S.A. In: *Incised Valleys in Time and Space* (Eds R.W. Dalrymple, D.A. Leckie and R.W. Tillman), *SEPM Spec. Publ.*, **85,** 239–280, Tulsa, OK.

Gingras, M.K., Pemberton, S.G. and **Saunders, T.** (1999) The ichnology of modern and Pleistocene brackish-water deposits at Willapa Bay, Washington: variability in estuarine settings. *Palaios*, **14,** 352–374.

Glumac, B., Berrios, L., Greer, L. and **Curran, H.A.** 2004. Holocene tufa-coated serpulid mounds from the Dominican Republic: depositional and diagenetic history, with comparison to modern serpulid aggregates from Baffin Bay, Texas. In: *11th Syposium on the Geology of the Bahamas and other Carbonate regions*, pp. 49–65. San Salvador, Bahamas.

Gunter, G. (1945) Studies of marine fishes of Texas. *Publ. Inst. Mar. Sci.*, **1,** 1–190.

Harris, P.T. 1994. Incised valleys and backstepping deltaic deposits in a foreland-basin setting, Torres Strait and Gulf of Papua, Australia. In: *Incised-Valley Systems: Origin and Sedimentary Sequences* (Eds R.W. Dalrymple, R. Boyd and B.A. Zaitlin), *SEPM Spec. Publ.*, **51,** 97–108, Tulsa, OK.

Hori, K. and **Saito, Y.** (2007) An early Holocene sea-level jump and delta initiation. *Geophys. Res. Lett.*, **34,** L18401.

Johnson, R.D. 1997. *The Facies, Environments of Deposition and Cyclicity of the Yates Formation, North Ward-Estes Field, Ward County, Texas*. Texas A&M University, College Station, TX, 79 pp.

Kendall, R.A., Mitrovica, J.X., Milne, G.A., Tornqvist, T.E. and **Li, Y.** (2008) The sea-level fingerprint of the 8.2 ka climate event. *Geology*, **36,** 423–426.

Land, L.S., Behrens, E.W. and **Frishman, S.A.** (1979) The ooids of Baffin Bay, Texas. *J. Sed. Petrol.*, **49,** 1269–1278.

Li, C., Wang, P., Fan, D. and **Yang, S.** 2006. Characteristics and formation of Late Quaternary incised-valley-fill sequences in sediment-rich deltas and estuaries: case studies from China. In: *Incised Valleys in Time and Space* (Eds R.W. Dalrymple, D.A. Leckie and R.W. Tillman), *SEPM Spec. Publ.*, **85,** 141–160, Tulsa, OK.

Lohse, E.A. (1956) Dynamic geology of the modern coastal region, northwestern Gulf of Mexico. In: *Finding Ancient Shorelines: A Symposium with Discussions* (Ed J.L. Hough), *SEPM Spec. Publ.*, **3,** 99–104.

Maddox, J., Anderson, J.B., Milliken, K.T., Rodriguez, A.B., Dellapenna, T.M. and **Giosan, L.** 2008. The Holocene evolution of the Matagorda and Lavaca estuary complex, Texas, USA. In: *Response of Upper Gulf Coast Estuaries to Holocene Climate Change and Sea-Level Rise* (Eds J.B. Anderson and A.B. Rodriguez), *Geol. Soc. Am. Spec. Pap.*, **443,** 105–119, Boulder, CO.

Mallinson, D., Riggs, S., Thieler, E.R., Culver, S., Farrell, K., Foster, D.S., Corbett, D.R., Horton, B. and **Wehmiller, J.F.** (2005) Late Neogene and Quaternary evolution of the northern Albemarle Embayment (mid-Atlantic continental margin, USA). *Mar. Geol.*, **217,** 97–117.

Martinsen, O.J. 1994. Evolution of an incised-valley fill, the Pine Ridge Sandstone of southeastern Wyoming, USA: systematic sedimentary response to relative sea-level change. In: *Incised-Valley Systems: Origin and Sedimentary Sequences* (Eds R.W. Dalrymple, R. Boyd and B.A. Zaitlin), *SEPM Spec. Publ.*, **51,** 109–128, Tulsa, OK.

Mattheus, C.R., Rodriguez, A.B., Greene, D.L., Simms, A.R. and **Anderson, J.B.** (2007) Control of upstream variables on incised-valley dimension. *J. Sed. Res.*, **77,** 213–224.

McBride, R.A., Taylor, M.J. and **Byrnes, M.R.** (2007) Coastal morphodynamics and chenier-plain evolution in southwestern Louisiana, USA: A geomorphic model. *Geomorphology*, **88,** 367–422.

McEwen, M.C. (1969) Sedimentary facies of the modern Trinity delta. In: *Holocene Geology of the Galveston Bay Area* (Eds R.R. Lankford and J.J.W. Rogers), pp. 53–77. Houston Geological Society, Houston.

McFarlan, E.J. (1961) Radiocarbon dating of Late Quaternary deposits, south Louisiana. *Geol. Soc. Am. Bull.*, **72,** 129–158.

Militello, A. 1998. *Hydrodynamics of wind-dominated, shallow embayments*, PhD Dissertation, Florida Institute of Technology, Melbourne, FL, 232 pp.

Miller, J.A. (1975) Facies characteristics of Laguna Madre wind-tidal flat. In: *Tidal Deposits: A Casebook of Recent Examples and Fossil Counterparts* (Ed. R.N. Ginsburg), pp. 67–73. Springer-Verlag, New York.

Milliken, K.T., Anderson, J.B. and **Rodriguez, A.B.** 2008a. A new composite Holocene sea-level curve for the northern Gulf of Mexico. In: *Response of Upper Gulf Coast Estuaries to Holocene Climate Change and Sea-Level Rise* (Eds J.B. Anderson and A.B. Rodriguez), *Geol. Soc. Am. Spec. Pap.*, **443,** 1–12, Boulder, CO.

Milliken, K.T., Anderson, J.B. and **Rodriguez, A.B.** 2008b. Record of dramatic Holocene environmental changes linked to eustasy and climate change in Calcasieu Lake, Louisiana, USA. In: *Response of Upper Gulf Coast Estuaries to Holocene Climate Change and Sea-Level Rise* (Eds J.B. Anderson and A.B. Rodriguez), *Geol. Soc. Am. Spec. Pap.*, **443,** 43–64, Boulder, CO.

Milliken, K.T., Anderson, J.B. and **Rodriguez, A.B.** 2008c. Tracking the Holocene evolution of Sabine Lake through the interplay of eustasy, antecedent topography, and sediment supply variations, Texas and Louisiana, USA. In: *Response of Upper Gulf Coast Estuaries to Holocene Climate Change and Sea-Level Rise* (Eds J.B. Anderson and A.B. Rodriguez), *Geol. Soc. Am. Spec. Pap.*, **443**. 65–88, Boulder, CO.

Morse, J.W., Cornwell, J.C., Arakaki, T., Lin, S. and **Huerta-Diaz, M.** (1992) Iron sulfide and carbonate mineral diagenesis in Baffin Bay, Texas. *J. Sed. Petrol.*, **62,** 671–680.

Morton, R.A. and **Kindinger, J.L.** (1998) Responses of coastal systems of Late Pleistocene and Holocene sea-level fluctuations Corpus Christi Region. *Gulf Coast Association of Geological Societies Annual Meeting, Field Trip Guide* pp. 1–29. Gulf Coast Association of Geological Societies, Corpus Christi, TX.

Morton, R.A., Paine, J.G. and **Blum, M.** (2000) Responses of stable bay-margin and barrier-island systems to Holocene sea-level highstands, Western Gulf of Mexico. *J. Sed. Res.*, **70,** 478–490.

Musgrove, M.L., Banner, J.L., Mack, L.E., Combs, D.M., James, E.W., Cheng, H. and **Edwards, R.L.** (2001) Geochronology of late Pleistocene to Holocene speleothems from central Texas: implications for regional paleoclimates. *Geol. Soc. Am. Bull.*, **113,** 1532–1543.

Nichols, M.M., Johnson, G.H. and **Peebles, P.C.** (1991) Modern sediments and facies model for a microtidal coastal plain estuary, the James Estuary, Virginia. *J. Sed. Petrol.*, **61,** 883–899.

Nordfjord, S., Goff, J.A., Austin, J.A.J. and **Gulick, S.P.S.** (2006) Seismic facies of incised-valley fills, New Jersey continental shelf: implications for erosion and preservation processes acting during latest Pleistocene–Holocene transgression. *J. Sed. Res.*, **76,** 1284–1303.

Nordt, L.C., Boutton, T.W., Jacob, J.S. and **Mandel, R.D.** (2002) C_4 plant productivity and climate-CO_2 variations in south-central Texas during the Late Quaternary. *Quatern. Res.*, **58,** 182–188.

Otvos, E.G. (2001) Assumed Holocene highstands, Gulf of Mexico: basic issues of sedimentary and landform criteria – discussion. *J. Sed. Res.*, **71,** 645–647.

Otvos, E.G. (2004) Holocene Gulf levels: recognition issues and an updated sea-level curve. *J. Coast. Res.*, **20,** 680–699.

Otvos, E.G. (2005) Numerical chronology of Pleistocene coastal plain and valley development; extensive aggradation during glacial low sea-levels. *Quatern. Int.*, **135,** 91–113.

Otvos, E.G. and **Howat, W.E.** (1996) South Texas Ingleside Barrier; coastal sediment cycles and vertabrate fauna. Late Pleistocene stratigraphy revised. *Trans. Gulf Coast Assoc. Geol. Soc.*, **46,** 333–344.

Paine, J.G. (1993) Subsidence of the Texas coast: inferences from historical and late Pleistocene sea levels. *Tectonophysics*, **222,** 445–458.

Payenberg, T.H.D., Boyd, R., Beaudoin, J., Ruming, K., Davies, S., Roberts, J. and **Lang, S.C.** 2006. The filling of an incised valley by shelf dunes – an example from Hervey Bay, east coast of Australia. In: *Incised Valleys in Time and Space* (Eds R.W. Dalrymple, D.A. Leckie and R.W. Tillman), *SEPM Spec. Publ.*, **85,** 87–98, Tulsa, OK.

Price, W.A. (1933a) Role of diastrophism in topography of Corpus Christi area, south Texas. *AAPG Bull.*, **17,** 907–962.

Price, W.A. (1933b) Reynosa problem of south Texas, and origin of Caliche. *AAPG Bull.*, **17,** 488–522.

Reimer, P.J., Baillie, M.G.L., Bard, E., Bayliss, A., Beck, J.W., Bertrand, C.J.H., Blackwell, P.G., Buck, C.E., Burr, G.S., Cutler, K.B., Damon, P.E., Edwards, R.L., Fairbanks, R.G., Friedrich, M., Guilderson, T.P., Hogg, A.G., Hughen, K.A., Kromer, B., McCormac, G., Manning, S., Ramsey, C.B., Reimer, R.W., Remmele, S., Southon, J., Stuiver, M., Talamo, S., Taylor, F.W., van der Plicht, J. and **Weyhenmeyer, C.E.** (2004) IntCal04 Terrestrial radiocarbon age calibration, 26-0 ka BP. *Radiocarbon*, **46,** 1029–1058.

Roberts, H.H., Fillon, R.H., Kohl, B., Robalin, J. and **Sydow, J.** 2004. Depositional architecture of the Lagniappe Delta: sediment characteristics, timing of depositional events, and temporal relationship with adjacent shelf-edge deltas. In: *Late Quaternary stratigraphic evolution of the northern Gulf of Mexico margin* (Eds J.B. Anderson and R.H. Fillon), *SEPM Spec. Publ.*, **79,** 143–188, Tulsa, OK.

Rodriguez, A.B. and **Meyer, C.T.** (2006) Sea-level variation during the Holocene deduced from the morphological and stratigraphic evolution of Morgan Peninsula, Alabama, USA. *J. Sed. Res.*, **76,** 257–269.

Rodriguez, A.B., Anderson, J.B. and **Simms, A.R.** (2005) Terrace inundation as an autocyclic mechanism for parasequence formation: Galveston Estuary, Texas, U.S.A. *J. Sed. Res.*, **75,** 608–620.

Rodriguez, A.B., Greene, D.L.J., Anderson, J.B. and **Simms, A.R.** 2008. Response of Mobile Bay and eastern Mississippi Sound, Alabama, to changes in sediment accomodation and accumulation. In: *Response of Upper Gulf Coast Estuaries to Holocene Climate Change and Sea-Level Rise* (Eds J.B. Anderson and A.B. Rodriguez), *Geol. Soc. Am. Spec. Pap.*, **443,** 13–30, Boulder, CO.

Rossetti, D.F. and **Junior, A.E.S.** (2004) Facies architecture in a tectonically influenced estuarine incised valley fill of Miocene age, northern Brazil. *J. S. Am. Earth Sci.*, **17,** 267–284.

Rusnak, G.A. (1960) Sediments of Laguna Madre, Texas. In: *Recent Sediments, Northwest Gulf of Mexico* (Eds F.P. Shepard, F.B. Phleger and T.H. Van Andel), pp. 153–196. American Association of Petroleum Geologist, Tulsa, OK.

Scott, R.W., Combes, J.M. and **Nissen, S.E.** (1998) High-precision chronostratigraphy of a late Pleistocene shelf-edge delta, Louisiana. *J. Sed. Res.*, **68,** 596–602.

Shepard, F.P. (1960) Rise of sea level along northwest Gulf of Mexico. In: *Recent Sediments, Northwest Gulf of Mexico* (Eds F.P. Shepard, F.B. Phleger and T.H. Van Andel), pp. 338–344. AAPG, Tulsa, OK.

Shepard, F.P. and **Moore, D.G.** (1960) Bays of central Texas coast. In: *Recent Sediments, Northwest Gulf of Mexico* (Eds F.P. Shepard, F.B. Phleger and T.H. Van Andel), pp. 117–152. American Association of Petroleum Geologist, Tulsa, OK.

Shideler, G.L. 1986. Seismic and physical stratigraphy of late Quaternary deposits, south Texas coastal complex. In: *Stratigraphic Studies of a Late Quaternary Barrier-Type Coastal Complex: Mustang Island-Corpus Christi Area, South Texas Gulf Coast* (Ed. G.L. Shideler), *US Geol. Surv. Prof. Pap.*, **1328-B,** 9–31.

Simms, A.R., Anderson, J.B., Taha, Z.P. and **Rodriguez, A.B.** 2006. Over-filled versus under-filled incised valleys: lessons from the Quaternary Gulf of Mexico. In: *Incised Valleys through Space and Time* (Eds R. Dalrymple, D. Leckie and R. Tillman), *SEPM Spec. Publ.*, **85,** 117–139.

Simms, A.R., Anderson, J.B., Milliken, K.T., Taha, Z.P. and **Wellner, J.S.** 2007a. Geomorphology and age of the oxygen isotope stage 2 (last lowstand) sequence boundary on the northwestern Gulf of Mexico continental shelf. In: *Seismic Geomorphology: Applications to Hydrocarbon Exploration and Production* (Eds R.J. Davies, H.W. Posamentier, L.J. Wood and J.A. Cartwright), *Geol. Soc. London Spec. Publ.*, **277,** 29–46, London.

Simms, A.R., Lambeck, K., Purcell, A., Anderson, J.B. and **Rodriguez, A.B.** (2007b) Sea-level history of the Gulf of Mexico since the Last Glacial Maximum with implications for the melting history of the Laurentide Ice Sheet. *Quatern. Sci. Rev.*, **26,** 920–940.

Simms, A.R., Anderson, J.B., Rodriguez, A.B. and **Taviani, M.** 2008. Mechanisms controlling environmental change within an estuary: Corpus Christi Bay, Texas, USA. In: *Response of Upper Gulf Coast Estuaries to Holocene Climate Change and Sea-Level Rise* (Eds J.B. Anderson and A.B. Rodriguez), *Geol. Soc. Am. Spec. Pap.*, **443,** 121–146, Boulder, CO.

Simms, A.R., Aryal, N., Yokoyoma, Y., Matsuzaki, H. and **DeWitt, R.** (2009). Insights on a proposed mid-Holocene highstand along the northwestern Gulf of Mexico from the evolution of small coastal ponds. *J. Sed. Res.*, **79**: 757–772.

Sperraza, M., Moore, J.N. and **Hendrix, M.S.** (2004) High-resolution particle size analysis of naturally occurring very fine-grained sediment through laser diffractometry. *J. Sed. Res.*, **74,** 736–743.

Sydow, J. and **Roberts, H.H.** (1994) Stratigraphic framework of a late Pleistocene shelf-edge delta, northeast Gulf of Mexico. *AAPG Bull.*, **78,** 1276–1312.

Tanner, W.F., Demirpolat, S., Stapor, F.W. and **Alvarez, L.** (1989) The ''Gulf of Mexico'' late Holocene sea level curve. *Trans. Gulf Coast Assoc. Geol. Soc.*, **39,** 553–562.

Thieler, E.R., Butman, B., Schwab, W.C., Allison, M.A., Driscoll, N.W., Donnelly, F.P. and **Uchupi, E.** (2007) A catastrophic meltwater flood event and the formation of the Hudson Shelf Valley. *Palaeogeogr. Palaeoclimatol. Palaeoecol.*, **246,** 120–136.

Thomas, M.A. and **Anderson, J.B.** 1994. Sea-level controls on the facies architecture of the Trinity/Sabine incised-valley system, Texas continental shelf. In: *Incised-Valley Systems: Origins and Sedimentary Sequences* (Eds R.W. Dalrymple, R. Boyd and B.A. Zaitlin), *SEPM Spec. Publ.*, **51,** 63–82.

Toomey, R.S.I., Blum, M. and **Valastro, S.V.** (1993) Late Quaternary climates and environments of the Edwards Plateau, Texas. *Global Planet. Change*, **7,** 299–320.

Tornqvist, T.E., Gonzalez, J.L., Newsom, L.E., Van der Borg, K., De Jong, A.F.M. and **Kurnik, C.W.** (2004a) Deciphering Holocene sea-level history on the US Gulf Coast: a high-resolution record from the Mississippi Delta. *Geol. Soc. Am. Bull.*, **116,** 1026–1039.

Tornqvist, T.E., Bick, S.J. and **Gonzalez, J.L.** (2004b) Tracking the sea-level signature of the 8.2 ka cooling event: new constraints from the Mississippi Delta. *Geophys. Res. Lett.*, **31,** L23309.

United States Geological Survey, 2009. National WATER INFORMATION SYSTEMS. Available at: http://waterdata.usgs.gov/nwis/.

Wright, E.E., Hine, A.C., Goodbred, S.L.J. and **Locker, S.D.** (2005) The effect of sea-level and climate change on the development of a mixed siliciclastic-carbonate, deltaic coastline: Suwanee River, Florida, U.S.A. *J. Sed. Res.*, **75,** 621–635.

Yang, B.C., Dalrymple, R.W. and **Chun, S.S.** (2005) Sedimentation on a wave-dominated, open-coast tidal flat, south-western Korea: summer tidal flat – winter shoreface. *Sedimentology*, **52,** 235–252.

Ye, L. and **Kerr, D.** (2000) Sequence stratigraphy of the middle Pennsylvanian Bartlesville Sandstone, northeastern Oklahoma: A case of an underfilled incised valley. *AAPG Bull.*, **84,** 1185–1204.

Yokoyama, Y., Nakada, M., Maeda, Y., Nagaoka, S., Okuno, J., Matsumoto, E., Matsushima, Y. and **Sato, H.** (1996) Holocene sea-level change and hydro-isostasy along the west coast of Kyushu, Japan. *Palaeogeogr. Palaeoclimatol. Palaeoecol.*, **123,** 29–47.

Yokoyama, Y., Esat, T.M., Lambeck, K. and **Fifield, L.K.** (2000) Last ice age millennial scale climate changes recorded in Huon Peninsula Corals. *Radiocarbon*, **42,** 383–401.

Yokoyama, Y., Purcell, A., Marshall, J.F. and **Lambeck, K.** (2006) Sea-level during the early deglaciation period in the Great Barrier Reef, Australia. *Global Planet. Change*, **53,** 147–153.

Zaitlin, B.A., Dalrymple, R.W. and **Boyd, R.** 1994. The stratigraphic organization of incised-valley systems associated with relative sea-level change. In: *Incised-Valley Systems: Origin and Sedimentary Sequences* (Eds R.W. Dalrymple, R. Boyd and B.A. Zaitlin), *SEPM Spec. Publ.*, **51,** 45–60.

Manuscript received 17 February 2009; revision accepted 4 September 2009